J. Fluid Mech. (1968), *vol.* 31, *part* 3, *pp.* 547–582
Printed in Great Britain

The form drag of two-dimensional bluff-plates immersed in turbulent boundary layers

By M. C. GOOD AND P. N. JOUBERT
Department of Mechanical Engineering, University of Melbourne

(Received 17 July 1967)

Measurements of the distributions of pressure on a bluff flat plate (fence) have been correlated with the characteristics of the smooth-wall boundary layer in which it is immersed. For zero pressure-gradient flows, correlations are obtained for the variation of form drag with plate height h which are analogous in form to the 'law of the wall' and the 'velocity-defect law' for the boundary-layer velocity profile. The data for adverse pressure-gradient flows is suggestive of a 'law of the wake' type correlation. Pressures on the upstream face of the bluff-plate are determined by a wall-similarity law, even for $h/\delta > 1$, and are independent of the pressure-gradient history of the flow; the separation induced upstream is apparently of the Stratford–Townsend type. The effects of the history of the boundary layer are manifested only in the flow in the rear separation bubble, and then only for $h/\delta > \frac{1}{2}$. The base pressure is also sensitive to free-stream pressure gradients downstream of the bluff-plate. The relative extent of upstream influence of the bluff-plate on the boundary layer is found to increase rapidly as h/δ decreases. One set of measurements of the mean flow field is also presented.

1. Introduction

The incompressible flow situation considered in this paper arises when a two-dimensional flat plate is attached normal to a long smooth wall on which a turbulent boundary layer has developed. The geometry of the situation is illustrated in figure 1. The main concern of the investigation is to relate the form drag of the bluff-plate† to the characteristics of the boundary layer in which it is immersed. Boundary layers with and without a history of streamwise pressure gradients are considered. It is assumed that the distance from the origin of the turbulent flow to the bluff-plate station is large compared with the region of upstream influence of the bluff-plate. No consideration is given to the change in skin friction on the smooth wall.

When approaching a new flow problem one naturally looks to the results of previous work of a similar nature for a guide as to what to expect. In this case, very few measurements of pressures experienced by bodies immersed in shear flow have been reported.

† Throughout this paper the two-dimensional flat plate is referred to as the 'bluff-plate' and the wall to which it is attached is called the 'smooth wall'.

However, the general nature of the flow over isolated bluff-bodies with sharp edges placed in unsheared streams (no upstream boundary) is well known. The thin boundary layers formed on the body are forced to separate at its sharp

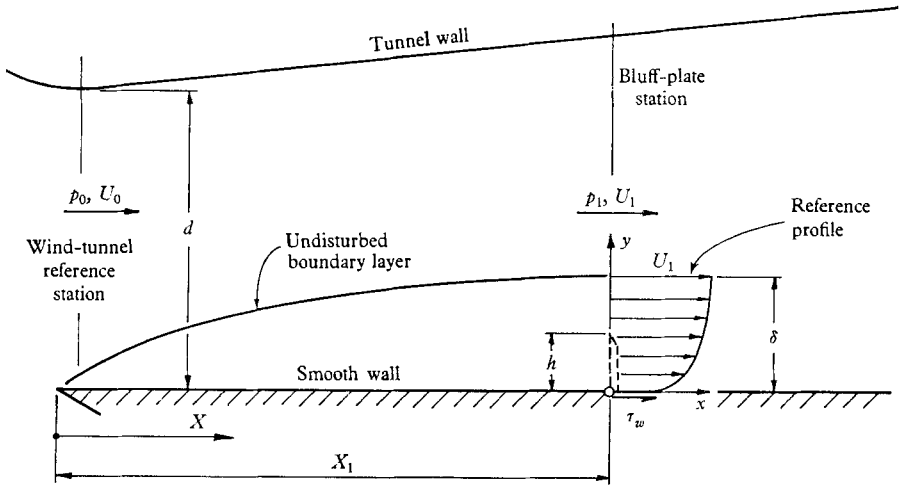

FIGURE 1. Experimental situation, and definition of variables.

edges, leaving the base of the body exposed to relatively sluggish separated flow—a uniform base pressure results. Provided this base pressure is known, pressures on the front face of the body may be calculated to good accuracy from free-streamline theory. The main problem in predicting the drag of such a bluff-body in a given situation is the determination of the base pressure, and this depends on the mechanics of the flow downstream of the body itself. For instance, Arie & Rouse (1956) showed that, if the process of periodic vortex formation downstream of a two-dimensional bluff-plate is prevented by the attachment of a long downstream splitter-plate, the drag coefficient of the bluff-plate is reduced from 2·1 to 1·4. The base pressure in this case is determined by the entrainment and reattachment processes along the shear layer dividing the free stream from the long separation bubble formed behind the bluff-plate.

The striking characteristic of bluff-body flows with no upstream boundary is that, for all Reynolds numbers above a few thousand, the form-drag coefficient is sensibly constant. This result may be interpreted thus: (*a*) the separation behaviour of the boundary layers formed on the body is determined by the body shape alone, and (*b*) the flow processes in the wake, which determine the base pressure, are dominated by the turbulence generated by the initial shearing between the free stream and the separated flow.

The association of the property 'constant drag coefficient' with the class of bodies of 'bluff shape' is very strong, and appears to have led some workers to expect that, when a bluff-body is attached to a wall and immersed in its boundary layer, the form drag will not be influenced by the fluid viscosity. Some have gone further and assumed that a drag coefficient may be defined which will have a constant value (independent of the size of the body in relation to the boundary-layer thickness, and independent of the shape of the approaching velocity

profile), provided some suitably 'representative' reference dynamic pressure is adopted.

Now it can be seen that the fluid viscosity may affect the drag in this situation because of its effect on (*a*) the distribution of incident momentum, and (*b*) the separation behaviour of the smooth-wall boundary layer, upstream of the bluff-body, under the influence of the bluff-body pressure field. However, Hoerner (1958) states that 'a small body, placed within a boundary layer, causes a drag component which corresponds, at least approximately, to the dynamic pressure of a layer limited by the height h of the body'. He goes on to define an 'independent' drag coefficient, $C_D = D/\bar{q}h$ (where D is the drag per unit length and $\bar{q}$ is the average dynamic pressure in the boundary layer between $y = 0$ and $y = h$), which supposedly has the constant value $C_D = 1{\cdot}25$ for a two-dimensional bluff-plate.

In a theory describing the action of isolated roughness elements, Morris (1954) employs a drag coefficient $C_{D_h} = D/q_h h$ (where q_h is the dynamic pressure in the boundary layer at $y = h$), with the implication that its value is characterized by the body shape alone. Townsend (1965*a*, *b*) introduced the same drag coefficient into a theory for the redevelopment of a boundary layer downstream of a line obstacle, but made no assumptions as to how its value might vary, except that it should be of order one.

It is common practice to extrapolate the results of wind-tunnel tests on, say, small-scale models of buildings, to the very much higher Reynolds numbers experienced by the real structure, because 'the flow around bluff bodies is independent of Reynolds number'. The validity of this assumption is not always tested as rigorously as it might be, particularly when some attempt is made to reproduce the shear profile of the real wind.

Only two direct measurements of the drag of a bluff-plate attached to a wall are known to the authors. In the first, Wieghardt (1953) attached various simple roughness elements to a smooth wall and measured the total change in resistance of the wall (i.e. the form drag of the element plus the change in skin-friction drag of the wall). Measurements were made with bluff-plates of several different heights, all immersed in the same zero pressure-gradient reference profile. Wieghardt hoped to make the results obtained under these fairly limited conditions applicable to flows at different Reynolds numbers, and to shear flows other than smooth-wall, zero pressure-gradient boundary layers, by suitable definitions of the drag coefficient and Reynolds number. To this end, the results were plotted in the form

$$\frac{D+\Delta W}{\bar{q}h} = f[\bar{u}h/\nu], \tag{1.1}$$

where D is the form drag per unit length of the bluff-plate and ΔW is the change in skin-friction drag of the smooth wall due to the disturbed flow pattern. The values of the mean velocity $\bar{u}$ and mean dynamic pressure $\bar{q}$ were calculated from the assumed reference profile at the bluff-plate station,

$$u/U_1 = (y/\delta)^{\frac{1}{7}}. \tag{1.2}$$

Wieghardt believed that the correlation scheme of (1.1) would be invalid only

for small values of h/δ. It will be shown later that, for the form drag at least, this correlation scheme is likely to be valid *only* for small h/δ.

Wieghardt's photographs of the flow over a two-dimensional bar of rectangular cross-section in a water-towing tank show that the mean flow in the separation bubble formed upstream of the bar was fairly steady, and that the length of this bubble increased as h/δ decreased. It is unlikely, therefore, that any drag coefficient can be defined which is strictly constant: if a constant drag coefficient is to obtain, the flow patterns for different values of h/δ should be geometrically similar. The photographs show that this is not so, although the means employed to vary the boundary-layer thickness (suction to reduce it, a screen of rods to increase it) may have influenced this result.

In a paper received after the present experiments had been completed, Plate (1964) proposes a method for predicting the changes in resistance measured by Wieghardt. He assumes that the form drag of a bluff-plate is independent of viscosity, and attempts to correlate his measurements of the form-drag coefficient $C_{D_1} = D/\frac{1}{2}\rho U_1^2 h$ (where U_1 is the free-stream velocity of the zero pressure-gradient flow) with h/δ only. He proposes the correlation

$$C_{D_1} = 1{\cdot}05(h/\delta)^{\frac{2}{7}}, \tag{1.3}$$

which, with equation (1.2) to represent the velocity profile, implies a value of $C_D = D/\bar{q}h = 1{\cdot}35$ compared with the value 1·25 quoted by Hoerner (1958) for this 'independent' drag coefficient. For a detailed critical analysis of this work the reader is referred to Good (1965). The results of the present investigation are compared with Plate's data in §4.11 of this paper.

All the work discussed above was basically concerned with zero pressure-gradient flows. Nash & Bradshaw (1967), however, require data on the form drag of an isolated roughness element which is immersed in a boundary layer with a history of streamwise pressure gradients, for the application of their theory for the 'magnification' of the profile drag of an aerofoil due to the element. They assume that these data may be obtained from measurements of the form drag of the element in a zero pressure-gradient boundary layer. This requires that the form drag be insensitive to the history of the shear flow and independent of local pressure gradients. The results of the present work indicate that these assumptions are not valid.

Summarizing, it can be said that, in drawing on the experience of bluff-body flows in free, unsheared streams when considering flow cases like the present one, perhaps insufficient attention has been paid to the basic differences between the flow processes involved. An attempt at rectifying this situation is made in the next section.

2. Analysis

The following is a résumé of the analysis which formed the basis of the authors' doubts about previous proposals concerning the drag of bluff-bodies attached to a wall. It also provided the rationale for the experimental program. The general experimental situation is illustrated in figure 1. Some of the important variables are also defined on the figure.

In general, one hopes to be able to predict the drag of a given bluff-plate from a knowledge of the characteristics of the boundary layer in which it is immersed. The complexity of the turbulent flow processes involved is such that an analytical solution is not possible in the present state of knowledge, and recourse must be made to experiment. The experiments should be designed in such a way that the results can be generalized sufficiently to be of use in situations other than those in which the experimental conditions are duplicated precisely. With this in mind, it would be convenient if the drag of a bluff-plate could be related to predictable or, at least, measurable mean-flow parameters of a single boundary-layer profile which is representative of the shear flow disturbed by the plate. The 'reference profile' which immediately suggests itself, and which is adopted in the present work, is that which would be measured at the bluff-plate station if the bluff-plate was absent.

An examination of the flow processes involved indicates how the history of the shear flow might affect the drag. If the experiments are initially restricted to conditions under which this history is adequately represented by mean-flow parameters of the reference profile, results of some general applicability should be obtained.

One can see immediately that successful correlations can be obtained for reference profiles with a history of zero pressure gradient. If the free-stream velocity U_1 does not vary with X, the drag D can depend only on h, X_1, d, U_1, ρ and μ, so that

$$D/\tfrac{1}{2}\rho U_1^2 h = f[h/X_1,\ U_1 X_1/\nu,\ d/h].\dagger \tag{2.1}$$

But the reference profile parameters δ/X_1 and $U_\tau/U_1 = (\tau_w/\rho U_1^2)^{\frac{1}{2}}$ are dependent only on the Reynolds number $U_1 X_1/\nu$. Also, provided d/h is large enough for blockage effects to be negligible, this parameter may be omitted. Hence equation (2.1) can be put in the desired form of correlation scheme,

$$D/\tfrac{1}{2}\rho U_1^2 h = f[h/\delta,\ U_\tau/U_1], \tag{2.2}$$

in which the drag is related entirely to mean-flow parameters of the reference profile. However, a more generally useful correlation is suggested by the following study of the flow processes.

2.1. *Flow model upstream of bluff-plate*

Upstream of the bluff-plate, an adverse pressure gradient will be produced by the deflexion of the flow by the bluff-plate. The boundary layer will be forced to separate from the smooth wall and will reattach on the front face of the bluff-plate, thereby enclosing a front separation bubble. Smoke-tunnel observations by the authors, and Wieghardt's (1953) photographs, show that the mean flow is steady. The streamline which separates from the wall, and divides the main flow from the separated flow, must therefore be the streamline which reattaches to the bluff-plate. These observations also show that the length of the front separation bubble is of the same order as the plate height, and about 60% of the upstream face of the bluff-plate is exposed to the separated flow.

† Square brackets are used throughout this paper to denote a functional dependence.

Within the separation bubble the flow reversed by the pressure gradient will be entrained into a mixing layer formed along the bubble boundary, only to be reversed again by the pressure rise near stagnation. Because of the already retarded state of the boundary layer, the motion thus set up in the bubble should be fairly slow, and incapable of sustaining large pressure differences. Hence, the general level of pressure over about 60 % of the upstream face of the bluff-plate will be determined by the separation pressure of the boundary layer.

Superimposed on this general pressure-level will be small variations due to the mechanics of the flow inside the bubble. For instance, the stagnation pressure of the boundary streamline will be greater than the separation pressure by the amount that the total pressure on this streamline is increased by turbulent mixing with the higher-velocity main flow. Note that this stagnation pressure is not necessarily the maximum pressure on the bluff-plate. It is possible that retardation of the higher-energy particles on streamlines above the dividing streamline will produce pressures on the plate higher than the stagnation pressure. In this case the flow up the plate from the reattachment point towards the pressure maximum would have to be sustained by gradients of shear stresses. Such a phenomenon is reported by Roshko & Lau (1965) in the reattachment region downstream of a backward-facing step. On the other hand, Sawyer (1960) found that the attachment point of a wall jet coincided with the point of maximum wall pressure.

An appreciation of the variables involved in determining the separation pressure achieved by the boundary layer, at least for plate heights large enough for the adverse pressure gradient caused by the plate to be impressed over the whole boundary-layer thickness, may be gained from studies of separation caused by a general retardation of the free stream. Newman's (1951) measurements in a separating boundary layer showed that, near separation, the flow was able to advance into the adverse pressure gradient mainly because of large streamwise gradients of the Reynolds direct stress $\rho\overline{u'^2}$, rather than by transverse gradients of the shear stress $-\rho\overline{u'v'}$. Newman also notes that the correlation measurements of Schubauer & Klebanoff (1950) indicate that the wall shear stress and surface pressure distribution in their separating boundary layer were determined by the distribution of the turbulent stress tensor *throughout* the layer, and not solely by local conditions near the surface. For large h/δ, then, it appears that the previous pressure-gradient history of the flow and, hence, the distributions of mean velocity and turbulent stress throughout the reference profile, might influence both the separation behaviour of the boundary layer in the bluff-plate pressure field, and the general character of the turbulent flow near the plate after separation has occurred. The variables required to specify these distributions would have to be known if the drag on the bluff-plate was to be determined uniquely.

A similar conclusion is reached concerning pressures on the bluff-plate outside the front separation bubble. These pressures result from the retardation of sheared flow, the momentum distribution of which will depend partly on the mean velocity distribution in the reference profile, and partly on the way this is modified during the pressure rise to separation and during mixing with the separated flow. The preceding discussion indicates that both these modifications

to the velocity profile could be influenced by the distribution of turbulence quantities throughout the reference profile.

2.2. *Flow model downstream of bluff-plate*

The streamline which separates from the tip of the bluff-plate will, if the mean flow is steady, reattach on the smooth wall. Arie & Rouse's (1956) experiments indicate that the rear separation bubble will be quite long: the bubble behind an isolated bluff-plate with a downstream splitter was 17 plate-heights long.

The base pressure will be closely related to the velocity of the accelerated flow near the tip of the bluff-plate, and this will depend on the general level of velocity in the upstream shear flow, and on the shape of the rear separation bubble. The steady-state bubble shape and base pressure may be regarded as resulting from a balance between the rate of entrainment of fluid from the bubble into the turbulent mixing layer along the long bubble boundary, and the rate of reversal of fluid back into the bubble by the pressure rise near reattachment (Korst 1956; Chapman, Kuehn & Larson 1957; Sawyer 1960, 1963). According to this interpretation, the base pressure will be affected by variables necessary to define the mean velocity distribution in the reference profile, and the turbulence structure involved in the mixing process along the rear separation bubble. In general, then, all the variables required to define uniquely the distributions of mean and turbulent velocities throughout the reference profile will have to be specified if the drag is to be determined uniquely.

2.3. *Restriction on class of shear flows*

So that a unique correlation between the drag and mean-flow parameters of the reference profile might be obtained, it was decided to limit the experiments to those shear flows for which an ordered relationship between the mean and turbulent distributions could be expected. The most obvious, and most restrictive limitation is to naturally developed, smooth-wall, zero pressure-gradient flows in which the free-stream turbulence level is small. The first stage of the investigation was therefore confined to zero pressure-gradient boundary layers.

Clauser (1954) demonstrated that the zero pressure-gradient boundary layer is only one of a family of 'equilibrium' flows in which the outer flow is self-preserving. Although simultaneous similarity in mean and turbulent distributions is not strictly possible, Clauser's (1956) results indicate that the departures from universality are small, and it is possible that the variables necessary to describe the mean-velocity profiles of equilibrium boundary layers will be sufficient to determine the turbulent distributions too. Coles (1956) found that a large class of boundary layers appear to be quasi-similar in the sense that the velocity can be represented as the sum of two terms, each of which shows similarity in the usual sense (see equation (2.3)). It might be expected that the distribution of other turbulence quantities would show the same quasi-similarity.

It was decided, therefore, that the scope of the investigations should be extended to include shear flows described adequately by Coles's correlation:

$$\frac{u}{U_\tau} = \frac{1}{\kappa}\log(yU_\tau/\nu) + C + \frac{\Pi[x]}{\kappa}w[y/\delta], \tag{2.3}$$

where κ and C are universal constants, w is a universal function of y/δ, and Π is a profile parameter. The conditions necessary for the establishment of such flows on smooth walls are, briefly, that streamwise changes in pressure should be fairly slow, the flow should not be too close to separation, and the free-stream turbulence level should be small. The accuracy of Coles's description of velocity profiles improves with increasing pressure gradients. The second stage of the investigations was consequently limited to moderate adverse pressure gradients.

2.4. *The possibility of wall-variable similarity*

Skin-friction measuring devices like the Preston tube (Preston 1954) and the sublayer fence (Head & Rechenberg 1962) require for their success that the pressures recorded depend only on the local wall shear stress and the fluid properties and not on the overall history of the flow. The Preston tube is intended to be immersed in the 'law of the wall' region of the velocity profile, but can be quite large in comparison with the boundary-layer thickness. Patel (1965) has shown that there are limitations on the usefulness of Preston tubes in strong pressure gradients. It is natural to speculate on the conditions under which wall similarity might be observed for pressures on the upstream face of the bluff-plates which are the concern of the present work. Of course, the flow pattern upstream of the three-dimensional Preston tube is quite different from the one described for a bluff-plate: the streamline which stagnates in or near the mouth of the Preston tube has its 'origin' in the undisturbed flow some distance from the wall; in the case of the bluff-plate, the stagnation streamline is the separation streamline of the upstream boundary layer.

If wall-variable similarity is to hold for bluff-plates, the upstream pressure gradients induced by the bluff-plate, and the separation behaviour of the boundary layer, under the action of these pressure gradients, must be independent of the history of the flow. Stratford (1959) and Townsend (1960, 1962) have postulated a type of rapid separation in which the Reynolds stresses are modified appreciably only in an inner 'equilibrium' layer. Because the local rates of production and dissipation of turbulent energy in this equilibrium layer are very high compared with the rate of energy gain by advection from the outer strata, the flow near the wall is entirely characterized by the initial wall shear stress and the local shear stress gradient $\partial\tau/\partial y$, and is otherwise independent of the history of the boundary layer.

If the adverse pressure gradient caused by the flow over the bluff-plate is assumed to be approximately constant, Townsend's (1962) theory indicates that the pressure rise to separation $(p_s - p_1)$ depends only on this constant pressure gradient, $\alpha_i = (1/\rho)\,dp/dx$, and the friction velocity for the reference profile, U_τ. Townsend's (1962) equation (5.2) becomes, in the present notation,

$$C_{s_\tau} = \frac{p_s - p_1}{\frac{1}{2}\rho U_\tau^2} = F[\alpha_i \nu / U_\tau^3]. \tag{2.4}$$

The pressure gradient α_i will depend on (at least) h, ρ, μ, and some velocity scale. For very large h/δ one would expect that the pressure distribution would be decided by the flow of the 'inviscid' free stream over the displacement surface

of the whole boundary layer. The appropriate reference velocity would then be U_1 and wall similarity would not be obtained. For small values of h/δ, however, the pressure distribution arises from the flow of turbulent, sheared fluid over the 'displacement surface' of the front separation bubble and the bluff-plate. Provided the pressure rise is sufficiently sudden for the flow near the wall to be of Townsend's 'equilibrium' type, the mean velocity and turbulence structure of the bulk of the flow involved should be characterized by the reference value of U_τ. This would lead to

$$\alpha_i \nu/U_\tau^3 = f[hU_\tau/\nu] \quad \text{only.} \tag{2.5}$$

The pressure rise to separation is then obtained from (2.4) as

$$C_{s_\tau} = f[hU_\tau/\nu]. \tag{2.6}$$

Under these conditions then, a wall law for pressures on the upstream face might be obtained.

Consideration of the flow in the rear separation-bubble leads to a similar conclusion concerning the base pressure. However, because of the influence of mean velocities near the tip of the bluff-plate, and the fact that there is more time available for the turbulence structure characterized by outer-flow variables to become involved in the flow in the long rear separation-bubble, one would expect that wall-similarity for the base pressure would break down at smaller plate heights than for the upstream-face pressures.

Summarizing then, provided the boundary layer has developed naturally, and any previous pressure gradients have been moderate, and provided the pressure rise induced by the bluff-plate is sudden, a wall-similarity law,

$$D/\tfrac{1}{2}\rho U_\tau^2 h = D/\tfrac{1}{2}\tau_w h = f[hU_\tau/\nu], \tag{2.7}$$

may be obtained for small values of h/δ.

As mentioned in the introduction, Wieghardt (1953) adopted the correlation scheme of (1.1) which may be written, for the form drag,

$$C_D = D/\bar{q}h = f[\bar{u}h/\nu]. \tag{2.8}$$

Provided h/δ is small enough for $\bar{u}/U_\tau$ and $\bar{q}/q_\tau$ (where $q_\tau = \frac{1}{2}\rho U_\tau^2$) to be calculated from the law of the wall, both these quantities will depend only on hU_τ/ν, and equation (2.8) reduces to the form of equation (2.7). However, Wieghardt believed that (1.1), and hence (2.8), would be strictly true only for large h/δ; the present arguments suggest it is only likely to be applicable for small h/δ.

2.5. *Correlation schemes*

The zero pressure-gradient correlation scheme, equation (2.2), may be put in the alternative forms

$$C_{D_\tau} = D/\tfrac{1}{2}\rho U_\tau^2 h = f[hU_\tau/\nu, h/\delta] \tag{2.9}$$

or

$$C_{D_\tau} = f[hU_\tau/\nu, U_\tau/U_1]. \tag{2.10}$$

The latter form is experimentally convenient and was adopted for the present experiments. The first argument was varied by changing the height of bluff-plates immersed in a given reference profile. U_τ/U_1 was varied by changing the free-stream velocity of the reference profile at the bluff-plate station.

For pressure-gradient flows, it was hoped that the history of the boundary layer would be adequately represented if Coles's profile parameter Π was added to the parameters in equation (2.10). That is,

$$C_{D_\tau} = f[hU_\tau/\nu,\ U_\tau/U_1,\ \Pi]. \tag{2.11}$$

To test this correlation scheme, hU_τ/ν was varied in a number of reference profiles characterized by a constant value of U_τ/U_1, but different values of Π.

3. Experimental equipment

3.1. *Wind tunnel*

The experiments were carried out in the low-speed, closed-circuit wind tunnel at the University of Melbourne. The original octagonal working section and diffuser of this tunnel (described by Perry & Joubert 1963) were modified to make the floor and ceiling parallel for a distance of 20 ft., with a clear distance between them of 4 ft. 1 in. A series of five turbulence-reducing screens was installed in the settling section upstream of the contraction, with the result that the free-stream turbulence level in the working section was reduced from approximately 1·0 to 0·3 %.

3.2. *Smooth-wall assembly*

The boundary layers were formed on a smooth wall, 22 ft. long by 4 ft. wide, placed vertically between the floor and ceiling of the working section, and projecting a short way into both the contraction and the diffuser. The wall consisted of a number of pressure-tapped panels, surfaced with laminated plastic, and could be moved bodily across the working section, or tilted at an angle to the air stream to produce streamwise pressure gradients. The gaps between the smooth-wall edges and the tunnel floor were sealed with felt strips.

3.3. *Bluff-plate assembly*

One of the smooth-wall panels could be replaced by a similar panel, 6 in. wide, through which a $\frac{1}{8}$ in. wide slot had been machined. Through this slot could be inserted the bluff-plate: a 6 in. wide by 3 ft. 7 in. long plate made from $\frac{1}{8}$ in. thick brass. A knife edge was machined along the exposed edge of the plate in order to simulate a plate of zero thickness. Any desired plate height from zero to $4\frac{1}{2}$ in. could be obtained by firmly clamping the plate, at the back of the panel. By suitable arrangements of the smooth-wall panels, the bluff-plate could be moved in 3 in. steps along the entire length of smooth wall. The gaps between the ends of the bluff-plate and the tunnel floor and ceiling were sealed with sheet metal end-pieces.

Forty-nine $\frac{1}{16}$ in. O.D. brass tubes were soldered into grooves machined in the plate surface. The surface irregularities were filled in with solder, which was smoothed over so that the final surface was flush with the plate surface. The piezometer holes were drilled through to the bore of the tubes with a spacing which increased progressively with distance from the knife edge. With this arrangement, a fairly detailed measurement of the pressure distribution on the upstream face could be obtained, even for a plate height of $\frac{1}{4}$ in. (7 exposed

pressure taps). Fewer taps were provided on the downstream face because the base pressure was known to be fairly uniform over the whole surface.

3.4. *Probes*

Two probes were used, in conjunction with a remotely controlled traversing system, for measurements of mean velocity and static-pressure profiles. The first probe, used for traverses of attached boundary layers, consisted of a flattened total-pressure tube, with an opening approximately 0·080 in. wide by 0·010 in. high, and two outrider static-pressure tubes of 0·8 mm diameter. The probe could be aligned with the flow direction with the aid of 'yaw' tubes on either side of the total-pressure tube.

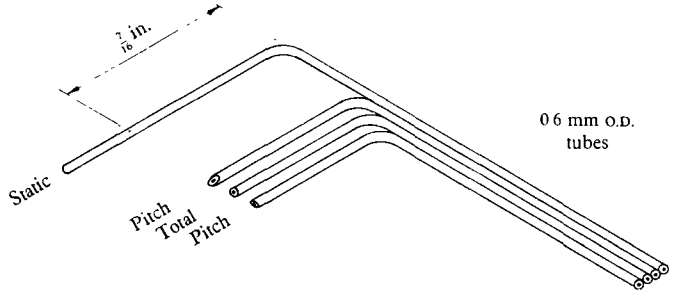

FIGURE 2. Detail of probe used in separated flow regions.

Measurements of the velocity and pressure fields in the separated flow near the bluff-plate were made with the second probe, a sketch of which is shown in figure 2. The 'pitch' tubes were made coplanar with the total-pressure and static-pressure tubes, in order to minimize the effects of high-velocity gradients on the measurements of flow direction.

4. Zero pressure-gradient experiments

The position in the tunnel of the smooth wall (without the bluff-plate fitted) was adjusted until the surface pressure taps, and measurements of the free-stream velocity at different stations, indicated that the pressure gradient was close to zero over the entire wall, except very near the leading edge.

4.1. *Boundary-layer results*

To demonstrate that a smooth-wall, 'equilibrium' flow had been established it was necessary to confirm that U_τ/U_1 and δ/X were functions of Reynolds number U_1X/ν only, and that Π was invariant. Mean velocity profiles were therefore measured, for a number of tunnel speeds, at five different X-stations.

The skin-friction parameter U_τ/U_1 was obtained by plotting the velocity profiles on a semi-logarithmic 'Clauser chart' (Clauser 1954). The logarithmic portion of the profile was compared with the family of straight lines represented by

$$\frac{u}{U_1} = 5{\cdot}75\frac{U_\tau}{U_1}\log_{10}(yU_1/\nu) + \frac{U_\tau}{U_1}\left(5{\cdot}75\log_{10}\frac{U_\tau}{U_1} + 5{\cdot}1\right). \tag{4.1}$$

Note that Coles's (1956) values for the universal constants κ and C in the logarithmic law of the wall have been used.

The variation of $C_f' = 2(U_\tau/U_1)^2$ with U_1X/ν is shown in figure 3(*a*), together with the results of direct measurements by a number of other workers. The correlation is generally satisfactory, although the values of C_f' at the lower

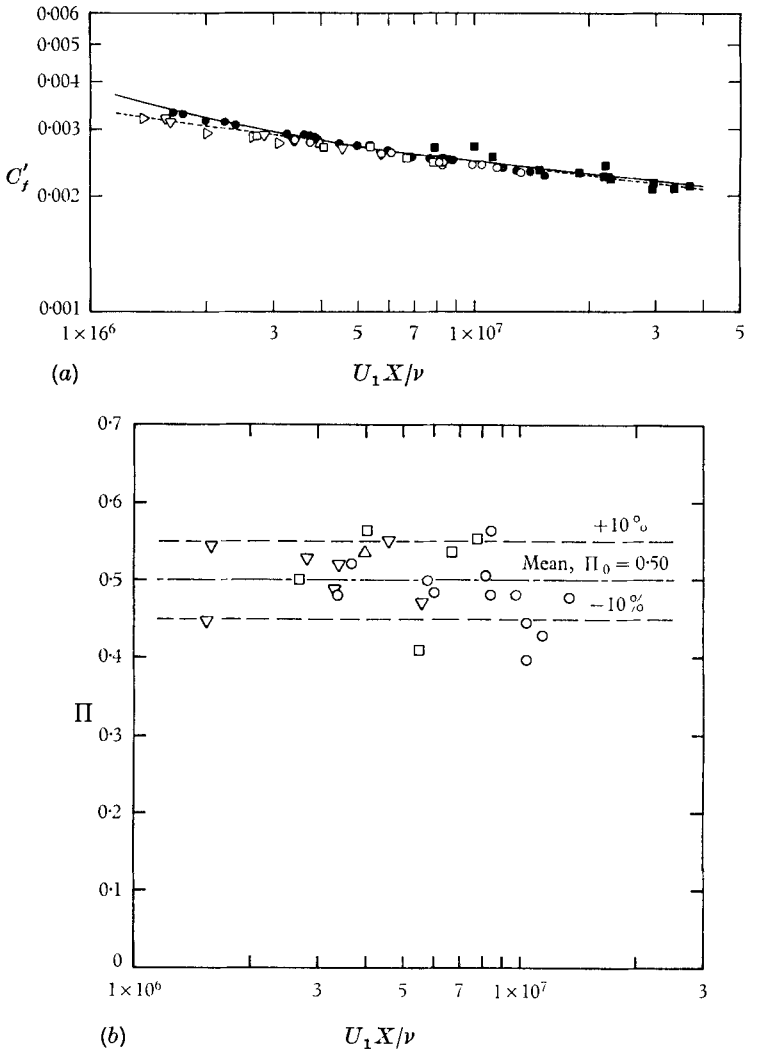

FIGURE 3. Calibration of smooth wall. Present work: ▷, $X = 43$ in.; ▽, 80 in.; △, 116 in.; □, 129 in.; ○, 177 in. (*a*) Comparison of skin-friction measurements with direct measurements of previous workers. ■, Kempf; ●, Shultz-Grunow; ——, Smith & Walker's direct measurement; ----, Smith & Walker's calculated resistance law based on asymptotic values of κ and C. All from Smith & Walker (1958). (*b*) Coles' profile parameter Π from zero pressure-gradient profiles.

Reynolds numbers tend to be lower than the direct measurements. They agree well, however, with the resistance law calculated by Smith & Walker (1958) from their 'asymptotic' values of κ and C.

Due to some unexplained inaccuracies in the outer part of the profiles, rather poor correlation of the 99 % boundary-layer thickness δ_{99} with Reynolds number

was obtained. However, the ratio of the velocity-defect length scale, $\Delta = \delta^* U_1/U_\tau$ (which is proportional to δ for an equilibrium layer of the Clauser type), to the accurately measured boundary-layer thicknesses of Smith & Walker was nearly constant over the whole Reynolds number range. This confirmed that the profiles were essentially in equilibrium. When a value for δ was required for use in the drag correlations, Smith & Walker's values were used.

Because of the apparent inaccuracies near the outer edge of the profiles, the values of Coles's profile parameter Π, shown in figure 3(*b*), were obtained from the solution of the equation

$$2\Pi - \ln(1+\Pi) = \kappa(U_1/U_\tau - C) - \ln(\kappa\delta^* U_1/\nu), \tag{4.2}$$

rather than from the alternative graphical construction described by Perry & Joubert (1963). It can be seen that there is no systematic change of Π with Reynolds number, but the scatter in the data is extensive. It was found that values of Π, obtained by either of the methods mentioned, were extremely sensitive to the assumed value of U_τ/U_1. For instance, from equation (4.2), an error $\epsilon(U_\tau/U_1)$ in U_τ/U_1 produces an error $\epsilon(\Pi)$ in Π given by

$$\frac{\epsilon(\Pi)}{\Pi} = -\frac{\kappa}{U_\tau/U_1}\frac{\Pi+1}{\Pi(2\Pi+1)}\frac{\epsilon(U_\tau/U_1)}{U_\tau/U_1}. \tag{4.3}$$

In the present case with $\kappa = 0{\cdot}4$, $\Pi \sim 0{\cdot}5$ and $U_\tau/U_1 \sim 0{\cdot}036$ an error of 1% in U_τ/U_1 produces an error of nearly 17% in Π. The scatter in the data for Π is therefore readily understood. However, this difficulty in obtaining accurate values for Π somewhat diminishes its usefulness as an experimental variable.

The average value of Π from the present profiles was $\Pi_0 = 0{\cdot}50$ compared with the value $\Pi_0 = 0{\cdot}55$ tentatively suggested by Coles.

4.2. *Two-dimensionality of flow*

The bluff-plate assembly was introduced 14 ft. 10 in. from the leading edge, and the plate height set at 4 in. The wall shear stress pattern, visualized by painting a thin suspension of titanium dioxide in kerosene on to the smooth wall and bluff-plate, showed no signs of three-dimensional effects except near the tunnel floor and ceiling. For this worst case (h = 4 in.), the flow in a central section, of aspect ratio equal to 6, was sensibly two-dimensional. It was concluded that centre-line measurements would be representative of truly two-dimensional flow.

4.3. *Blockage effects*

When a body is tested in a wind tunnel, the constraining effect of the tunnel walls causes velocities near the body to be higher than they would be in an infinite stream. It is usually assumed (for isolated bodies in a uniform stream) that the effect on the drag is similar to a simple increase in the approach velocity of the corresponding unbounded stream. However, this concept is of doubtful applicability in the present case, where the characteristics of the shear flow play a large part in determining the drag. What the effect of blockage might be on these characteristics, and on the turbulent flow processes determining the drag, can only be surmised at present. It is apparent that the variable d/h in equation (2.1) is as much a primary variable as the others in this equation as

far as the drag is concerned. No simple 'correction' may be made without regard to the shear flow.

It can be expected that the base-pressure component of the drag will be most affected by the local increase in velocities due to blockage, because the displacement thickness of the rear separation-bubble causes the greatest blockage. Arie & Rouse (1956) applied a correction only to the base pressure of a bluff-plate with a downstream splitter (which is not subject to the complications of upstream shear). Even in this case an exact correction could not be made: Arie & Rouse represented the shape of the *measured* separation bubble analytically, and calculated the correction using potential-flow theory, assuming that the bubble shape was unaffected by blockage. The order of magnitude of the maximum error due to blockage effects, in the present experiments, may be estimated from the fact that, with $d/h = 12$, Arie & Rouse applied a correction of about 9·5% to the base pressure. In the present experiments, the minimum value of d/h was 9; a maximum error due to blockage of about 10 to 15% could be expected.

For the reasons noted, no correction was applied to the present results. However, it is thought that the conclusions drawn about the effect of the boundary-layer characteristics on the drag coefficient are unlikely to be invalidated by blockage effects.

4.4. *Upstream influence of bluff-plate*

As a preliminary investigation, the distributions of wall pressure upstream of bluff-plates of six different heights were measured, in order to determine the extent of upstream influence of the plate, and to see whether it varied appreciably. The Reynolds number U_1X_1/ν was approximately the same for all the tests.

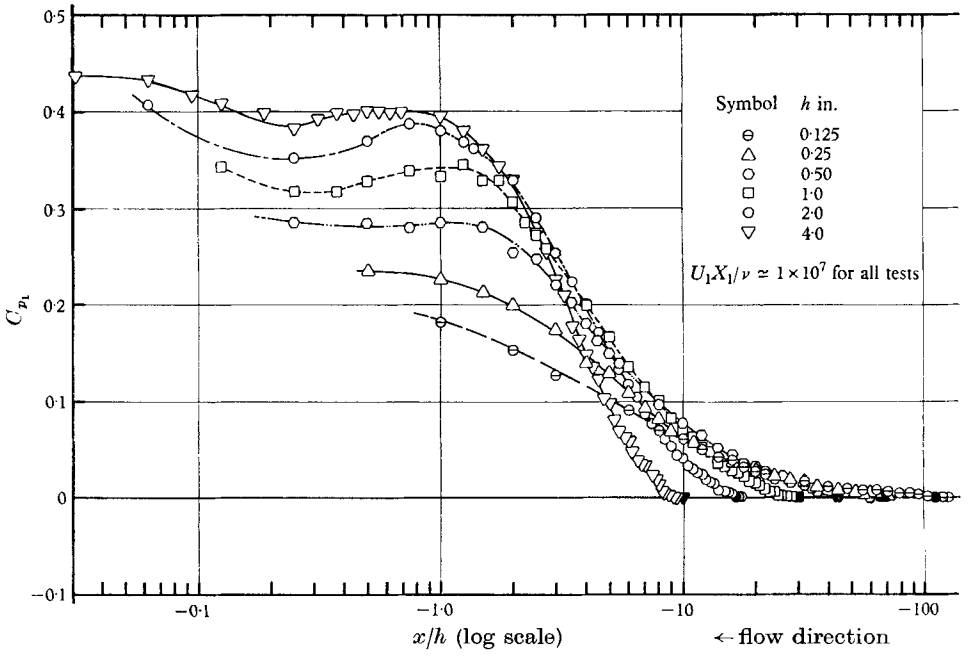

FIGURE 4. Surface pressure distributions upstream of bluff-plate. Filled symbols indicate beginning of region of upstream influence.

The most striking feature of these distributions, shown in figure 4, was the rapid increase in the relative extent of upstream influence as the plate height was

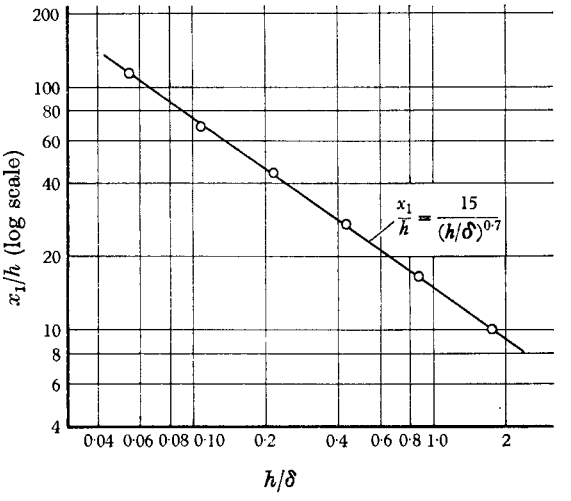

FIGURE 5. Extent of upstream influence of bluff-plate.
$U_1 X_1/\nu \simeq 1 \times 10^7$.

reduced. The variation of the relative distance upstream of the bluff-plate at which the wall pressure started to rise because of the plate (x_1/h) is shown in figure 5. The log–log plot shows that the variation, at this particular Reynolds number, is well expressed by

$$x_1/h = 15(h/\delta)^{-0.7}. \tag{4.4}$$

Apparently the disturbance to the boundary layer due to the bluff-plate is relatively more severe if the bulk of the shear flow which is actually disturbed by the plate (i.e. that part of the reference profile between $y = 0$ and $y = h$, say) is initially more retarded.

4.5. *Measurements of form drag*

The skin-friction law which had been established,

$$U_\tau/U_1 = f[U_1 X/\nu], \tag{4.5}$$

was used to predict the values of the unit Reynolds number at the tunnel reference station (U_1/ν) which would give $U_\tau/U_1 = 0{\cdot}0348$, $0{\cdot}0360$ and $0{\cdot}0375$ at $X =$ 14 ft. 10 in. These values were confirmed by profile measurement at this station (with $h = 0$), and represented the range of U_τ/U_1 which could conveniently be measured at this station.

Measurements were made of the distributions of pressure on bluff-plates of heights varying between $\frac{1}{8}$ in. and 4 in., at each value of U_τ/U_1.

4.6. *Dependence of C_{D_1} on outer-flow variables*

In the previous work by Plate (1964) it was assumed that the drag coefficient based on the free-stream dynamic pressure $C_{D_1} = D/\frac{1}{2}\rho U_1^2 h$ is uniquely related to h/δ. The present results for this drag coefficient are plotted in figure 6, and it is

apparent that C_{D_1} depends also on U_τ/U_1, except possibly for $h/\delta > 1$, in accordance with the general correlation

$$C_{D_1} = f[h/\delta,\ U_\tau/U_1], \tag{4.6}$$

given before as equation (2.2).

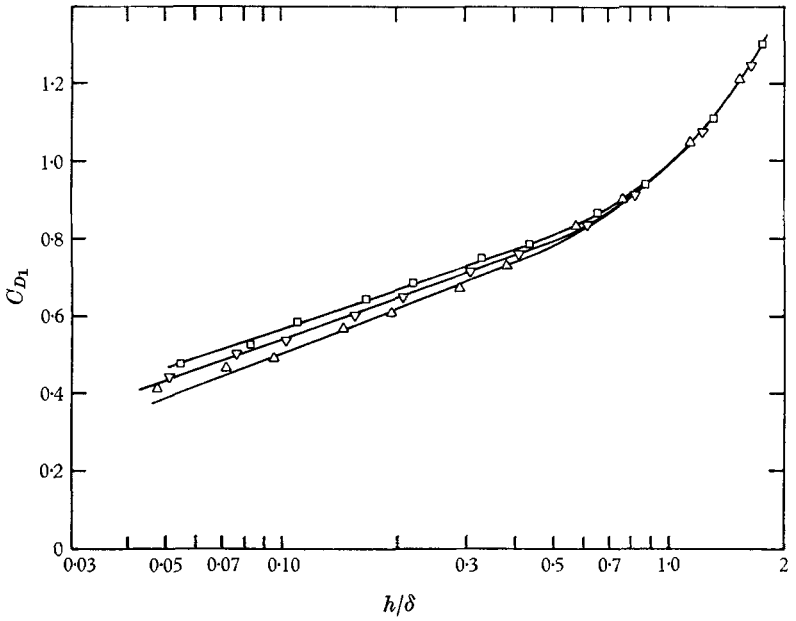

FIGURE 6. Plot showing dependence of C_{D_1} on outer-flow variables. □, $U_\tau/U_1 = 0{\cdot}0348$; ▽, 0·0360; △, 0·0375.

It can be seen that, over a considerable range of plate heights, the drag coefficient varies logarithmically with plate height, the slope of the semi-log line being different for each value of U_τ/U_1.

4.7. *Local-variable similarity*

It was suggested in §2.4 that, for small h/δ, the drag might depend only on the local variables ρ, ν and U_τ and the plate height h, so that

$$C_{D_\tau} = f[hU_\tau/\nu]. \tag{4.7}$$

The results are plotted in this form in figure 7 and it can be seen that there is, in fact, quite a large region of local-variable similarity (a 'wall law') in which the drag coefficient is given by

$$C_{D_\tau} = 277 \log_{10}(hU_\tau/\nu) - 268. \tag{4.8}$$

Referring to the argument in §2.4, it appears that the pressure rise, due to this disturbance *within* the boundary layer, is relatively sudden, and local rates of production and dissipation of turbulent energy dominate the separation process, and the flow balance in each separated region. Apparently there is insufficient time, before separation of the boundary layer, for the effects of the turbulence structure in the outer flow to diffuse downwards and affect the flow near the plate.

A wall law which is logarithmic in form suggests the following behaviour: when the plate height is comparable to the thickness of the viscous sublayer, changes in plate height produce changes in pressure on the plate which depend

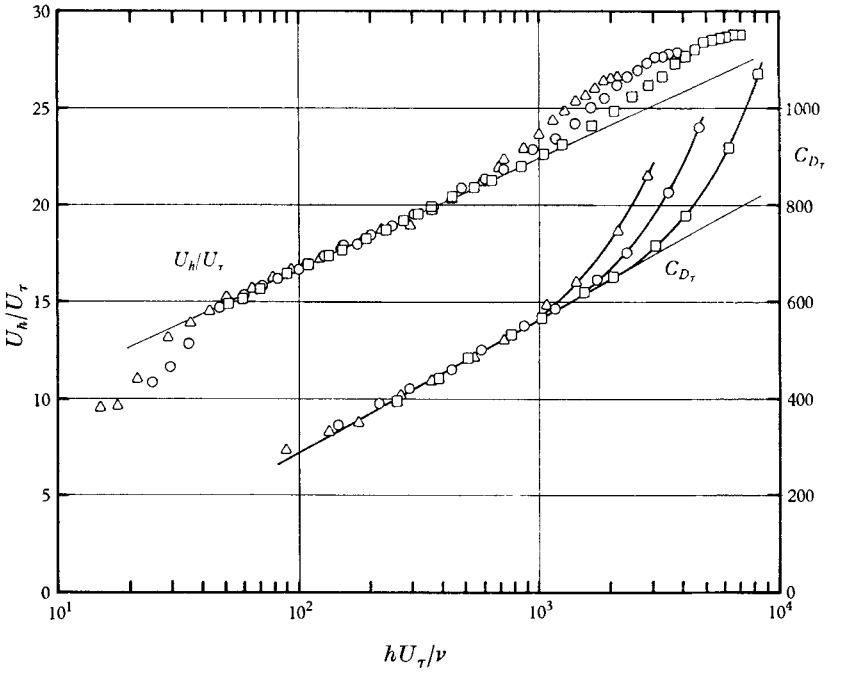

FIGURE 7. Wall similarity in mean-velocity and form-drag correlations. □, $U_\tau/U_1 = 0{\cdot}0348$, ○, 0·0360; △, 0·0375.

on the sublayer thickness. As the plate height increases further, and becomes large compared with the sublayer, the mechanism determining the flow pattern changes, so that further changes of pressure with plate height are no longer influenced by the sublayer thickness. The length scale for the viscous sublayer is ν/U_τ, so the above condition can be expressed formally by

$$(1/q_\tau)(D/h) = f[hU_\tau/\nu]$$

but

$$\frac{1}{q_\tau}\frac{\partial(D/h)}{\partial h} = \frac{U_\tau}{\nu}\frac{\partial f}{\partial(hU_\tau/\nu)} \neq f_1[\nu/U_\tau], \tag{4.9}$$

where D/h is the average of the pressure differentials over the bluff-plate. The form of the derivative is therefore restricted, the only allowable form being

$$\frac{\partial f}{\partial(hU_\tau/\nu)} = A(hU_\tau/\nu)^{-1}, \tag{4.10}$$

where A is a universal constant for zero pressure-gradient flows.

Integration of equation (4.10) yields

$$C_{D_\tau} = f[hU_\tau/\nu] = A\log(hU_\tau/\nu) + B, \tag{4.11}$$

where B is also a universal constant. This equation is in the same form as the empirical result, equation (4.8).

The above argument to establish the logarithmic variation of drag coefficient is analogous to that given by Rotta (1962) to explain the shape of the turbulent boundary-layer velocity profile. The analogous variation of C_{D_τ} and U_h/U_τ with hU_τ/ν is demonstrated in figure 7.

4.8. '*Drag-defect*' *law*

It will be recalled that the velocity profiles shown in figure 7 are of the form

$$\frac{U_h}{U_\tau} = \frac{1}{\kappa}\log(hU_\tau/\nu) + C + \frac{\Pi_0}{\kappa} w[h/\delta] \tag{4.12}$$

and may be correlated by the 'velocity-defect' law

$$\frac{u(h)-u(\delta)}{U_\tau} = \frac{U_h - U_1}{U_\tau} = f[h/\delta]. \tag{4.13}$$

Inspection of the curves representing the variation of the drag coefficient C_{D_τ} in figure 7 indicates that each deviation from the logarithmic wall law is of similar shape, and suggests that, by analogy with the velocity profiles, the drag coefficient might be given by

$$C_{D_\tau} = A\log(hU_\tau/\nu) + B + P.\phi[h/\delta], \tag{4.14}$$

where A, B and P are constants for zero pressure-gradient flows, and ϕ is a universal function of h/δ. The drag coefficients should then follow a 'drag-defect' law of the form

$$C_{D_\tau}(h) - C_{D_\tau}(\delta) = F[h/\delta]. \tag{4.15}$$

h/δ	$P.\phi[h/\delta]$	h/δ	$P.\phi[h/\delta]$
0–0·4	0	1·2	106
0·5	6	1·3	128
0·6	14	1·4	153
0·7	24	1·5	179
0·8	37	1·6	207
0·9	51	1·7	236
1·0	67	1·8	268
1·1	86		

TABLE 1. Tentative values for the proposed universal drag-deviation function for zero pressure-gradient flows

The data of figure 7 are replotted in defect form in figure 8, and the defect law is confirmed, apparently over the whole range of h/δ tested. The deviation from the log law occurs between $h/\delta = 0{\cdot}4$ and $h/\delta = 0{\cdot}5$. Tentative values for $P.\phi[h/\delta]$ are given in table 1.

The drag-defect law is a further demonstration that changes in pressure on the bluff-plate with changes of plate height are determined independently of the viscosity.

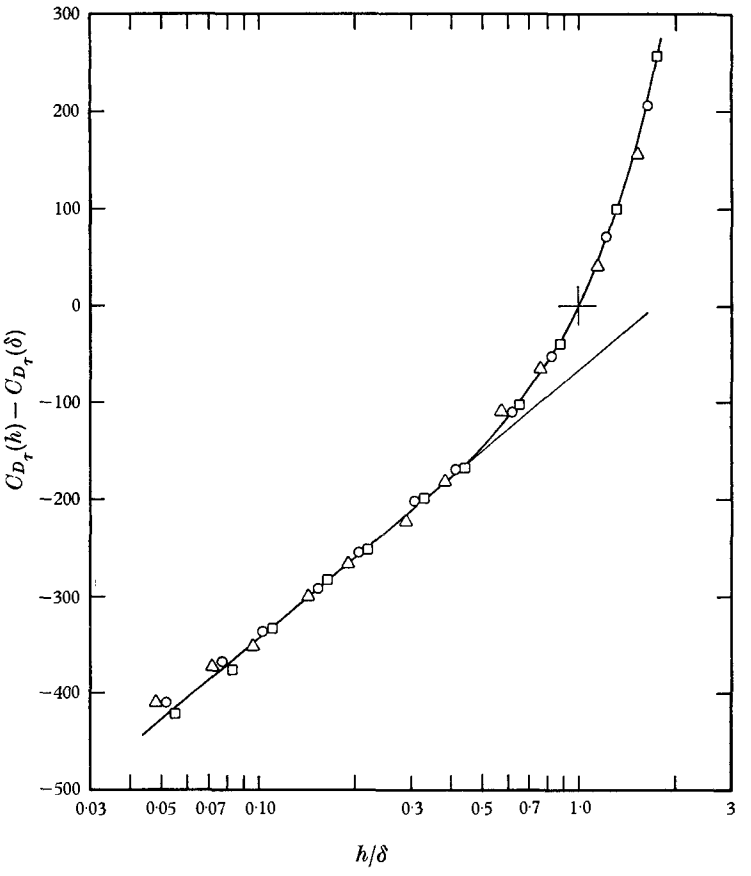

FIGURE 8. 'Drag-defect' law. □, $U_\tau/U_1 = 0{\cdot}0348$; ○, 0·0360; △, 0·0375.

4.9. *Contributions to drag from front and rear faces*

In figure 9, the base-pressure coefficient, $C_{b_\tau} = (p_b - p_1)/q_\tau$, and the contribution to the drag coefficient from the front face, $C_{u_\tau} = C_{D_\tau} + C_{b_\tau}$, are plotted separately. The average pressure on the upstream face follows a wall law over almost the entire range of h/δ tested. The distortion of the pressure distribution near the plate tip, caused by the requirement that $p = p_b$ at $y = h$, has a noticeable effect on C_{u_τ} for only the largest plate heights.

Thus, mean velocities and the turbulence structure which are characterized by U_1 and δ affect the drag only through their influence on the flow in the rear separation bubble. This behaviour is in accordance with the suggestions made in §2; however, the range of h/δ for which the front-face pressures follow a wall law is remarkable, and was quite unexpected.

The equations for the variation of C_{u_τ} and C_{b_τ} in the wall-law regions are

$$C_{u_\tau} = 125 \log_{10}(hU_\tau/\nu) - 121, \tag{4.16}$$

$$-C_{b_\tau} = 152 \log_{10}(hU_\tau/\nu) - 147. \tag{4.17}$$

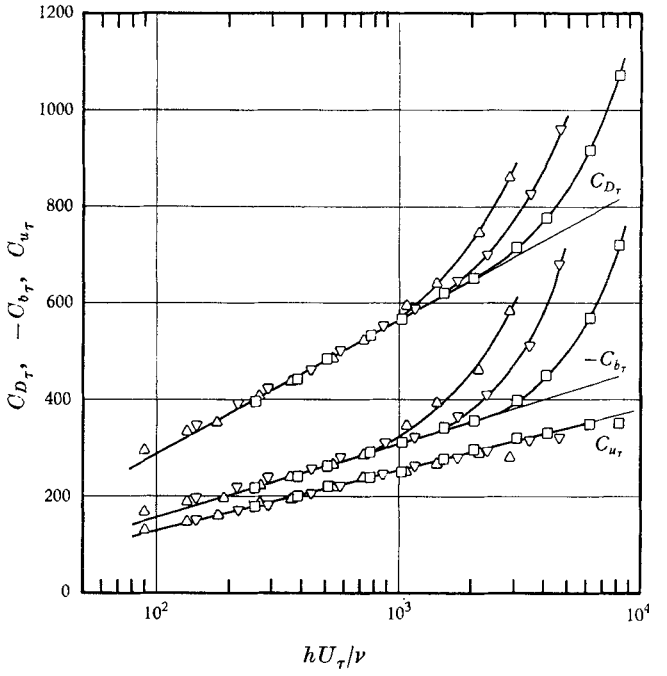

FIGURE 9. Segregation of drag coefficients into upstream and base-pressure components. □, $U_\tau/U_1 = 0{\cdot}0348$; ▽, 0·0360; △, 0·0375.

4.10. *The drag coefficients C_D and C_{D_h}*

As mentioned in the introduction, a number of workers have utilized the drag coefficients $C_D = D/\bar{q}h$ and $C_{D_h} = D/q_h h$ with the implication that their values are roughly constant for a given bluff-body. The variation of these drag coefficients with hU_τ/ν has been computed from the following generalizations of the experimental data.

Reference profile:

$$\left.\begin{aligned} u/U_\tau &= yU_\tau/\nu \quad (0 \leqslant yU_\tau/\nu \leqslant 11{\cdot}12) \\ &= 2{\cdot}5\ln(yU_\tau/\nu) + 5{\cdot}1 + 1{\cdot}375w[y/\delta] \quad (11{\cdot}12 < yU_\tau/\nu \leqslant \delta U_\tau/\nu) \\ &= U_1/U_\tau \quad (\delta U_\tau/\nu < yU_\tau/\nu). \end{aligned}\right\} \tag{4.18}$$

Drag coefficient:

$$C_{D_\tau} = 277\log_{10}(hU_\tau/\nu) - 268 + P.\phi[h/\delta]. \tag{4.19}$$

The function $w[y/\delta]$ has been tabulated by Coles (1956); the drag deviation function $P.\phi[h/\delta]$ is given in table 1. The results of the calculations are shown in figure 10, and it is apparent that the values of C_D and C_{D_h} may vary quite widely.

The drag coefficient defined in the present work, C_{D_τ}, has the advantage over C_D and C_{D_h} of being characterized by a single parameter, hU_τ/ν, up to $h/\delta \sim \frac{1}{2}$. Because of the dependence in their definition on the velocity distribution of the reference profile, C_D and C_{D_h} deviate from the wall-similarity law at much lower values of h/δ (viz. $h/\delta \sim \frac{1}{6}$).

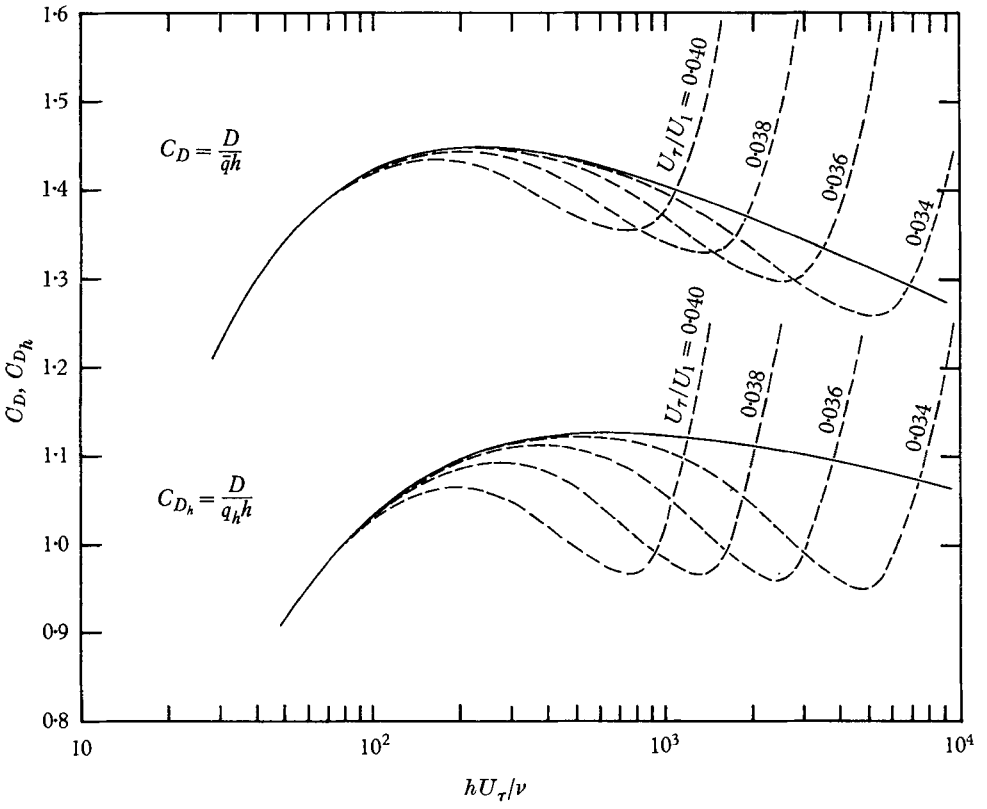

FIGURE 10. Test of invariance of the drag coefficients C_D and C_{D_h}. Full lines represent wall-similarity relationship.

4.11. *Comparison with previous work*

As mentioned before, Plate (1964) attempted to correlate measurments of C_{D_1}, made at various boundary-layer Reynolds numbers, with h/δ only. The present results show that this drag coefficient depends on the Reynolds number as well as h/δ (figure 6), and this may account for some of the scatter in his data.

Plate's results are all for $h/\delta < 0{\cdot}5$ and should therefore be correlated by the wall law $C_{D_\tau} = f[hU_\tau/\nu]$. Unfortunately the Reynolds number is not amongst the information given by Plate. However, it can be calculated from the quoted values of δ, which he worked out using

$$\delta/X_1 = 0{\cdot}37(U_1 X_1/\nu)^{-\frac{1}{5}}. \tag{4.20}$$

For consistency with Plate's approach, values of U_τ/U_1 for his experiments have been calculated by the authors, using Blasius's skin-friction law (Schlichting 1962):

$$(U_\tau/U_1)^2 = 0{\cdot}0296(U_1 X_1/\nu)^{-\frac{1}{5}}. \tag{4.21}$$

Plate's original data are plotted, in semi-log form, in figure 11 (*a*), to a fairly large scale. In figure 11 (*b*) the results of the authors' calculations of C_{D_τ} and hU_τ/ν from these data are plotted to a similar scale, together with the results of the present experiments. The agreement is quite good, and the scatter is no

worse than in the original data. This is encouraging because errors would have been introduced into the calculations by using rounded-off values of the original data, and by the doubtful accuracy of equation (4.21) in representing the variation of skin friction in Plate's experiments.

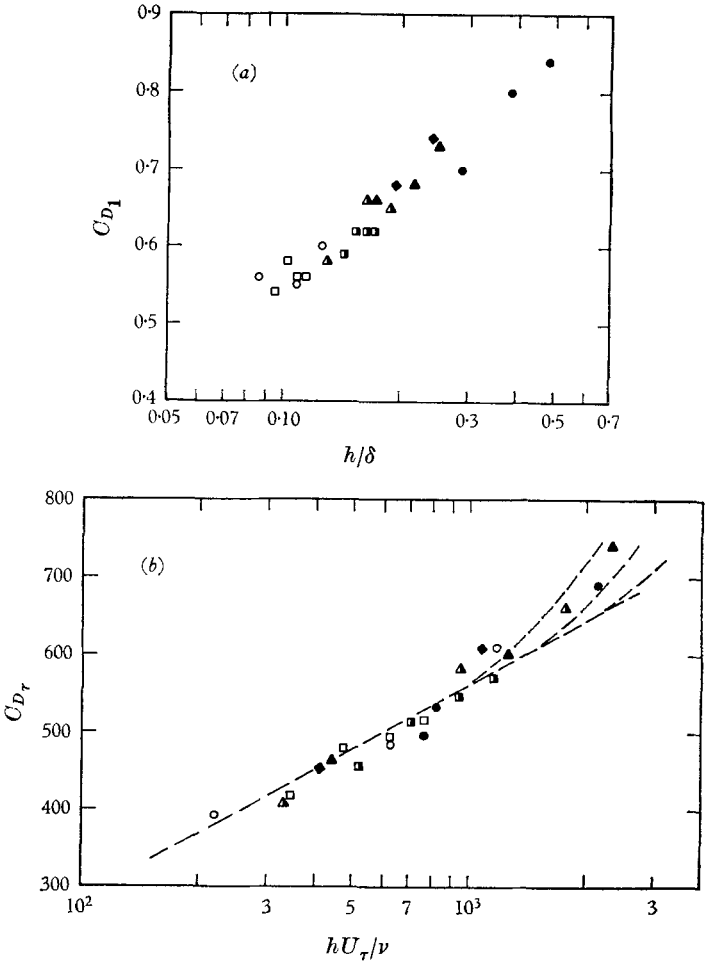

FIGURE 11. Comparison of present results with data of Plate (1964): ●, series 1 (h = 2 in.); ◆, 1 (1 in.); ○, 2 (1 in.); ◭, 2 (1·5 in.); ▲, 2 (2 in.); ◨, 3 (1·5 in.); □, 3 (1 in.). (*a*) Semi-log plot of Plate's original data. (*b*) Data expressed in wall-law form. – – – –, present results

Another result quoted by Plate, and used in the theory of his paper, is the proportionality of drag and base-pressure coefficients. The present results for C_{D_1} are plotted against the base-pressure coefficient $C_{b_1} = (p_b - p_1)/\frac{1}{2}\rho U_1^2$ in figure 12, together with Plate's data. The proportionality of the two coefficients is confirmed in the wall-law region only, the constant of proportionality suggested by the present data being $-1{\cdot}82$ compared with Plate's value of $-1{\cdot}65$. Because of the consistency of the present results, it is thought that any differences from Plate's data are due to errors and inconsistencies in defining the reference static pressure p_1 for the latter.

Plate also found that a drag coefficient C_{D_m}, based on the maximum pressure difference over the bluff-plate, was approximately constant for all the plates tested; viz.

$$C_{D_m} = \frac{D}{(p_m - p_b)h} \simeq 0{\cdot}95. \tag{4.22}$$

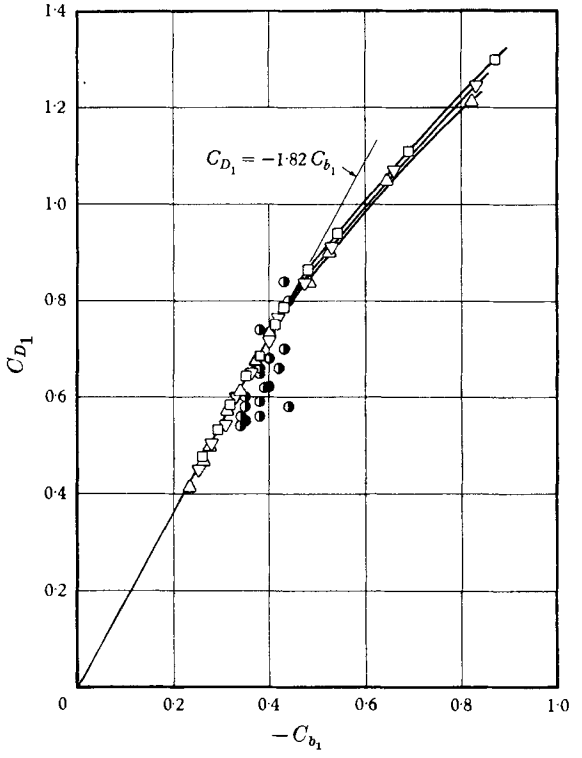

FIGURE 12. Proportionality of drag and base-pressure coefficients in wall-law region. ◑, Plate (1964). Present results: □, $U_\tau/U_1 = 0{\cdot}0348$; ▽, 0·0360; △, 0·0375.

This implies that the shape of the pressure distribution, when normalized by the maximum pressure differential, was approximately the same for all plates. He shows normalized pressure distributions measured on three bluff-plates at one X-station, and claims to detect slight changes in the shape of the distribution with free-stream velocity (i.e. with U_τ/U_1). The authors believe that the accuracy of the pressure measurements was not sufficient to justify this conclusion. Also, similarity with hU_τ/ν, rather than U_τ/U_1, would be expected. Values of C_{D_m} calculated from the present results are fairly constant over the whole range of plate heights, the average value being 0·945, which agrees well with Plate's figure of 0·95. However, the normalized pressure distributions are not strictly invariant, as is shown in the next section.

4.12. *Distribution of pressure on the bluff-plate*

In the discussion of the drag-coefficient results it was shown that the logarithmic variation of drag coefficient can be explained if changes in the average pressure difference D/h are determined independently of ν/U_τ. The same is true of the

individual pressures contributing to the average. Thus, in the wall-law region,

$$C_{p_\tau} = (p - p_1)/q_\tau = f[hU_\tau/\nu, y/h], \tag{4.23}$$

and, at each value of y/h,

$$C_{p_\tau} = g_1[y/h] \log (hU_\tau/\nu) + g_2[y/h], \tag{4.24}$$

where g_1 and g_2 are arbitrary functions of y/h.

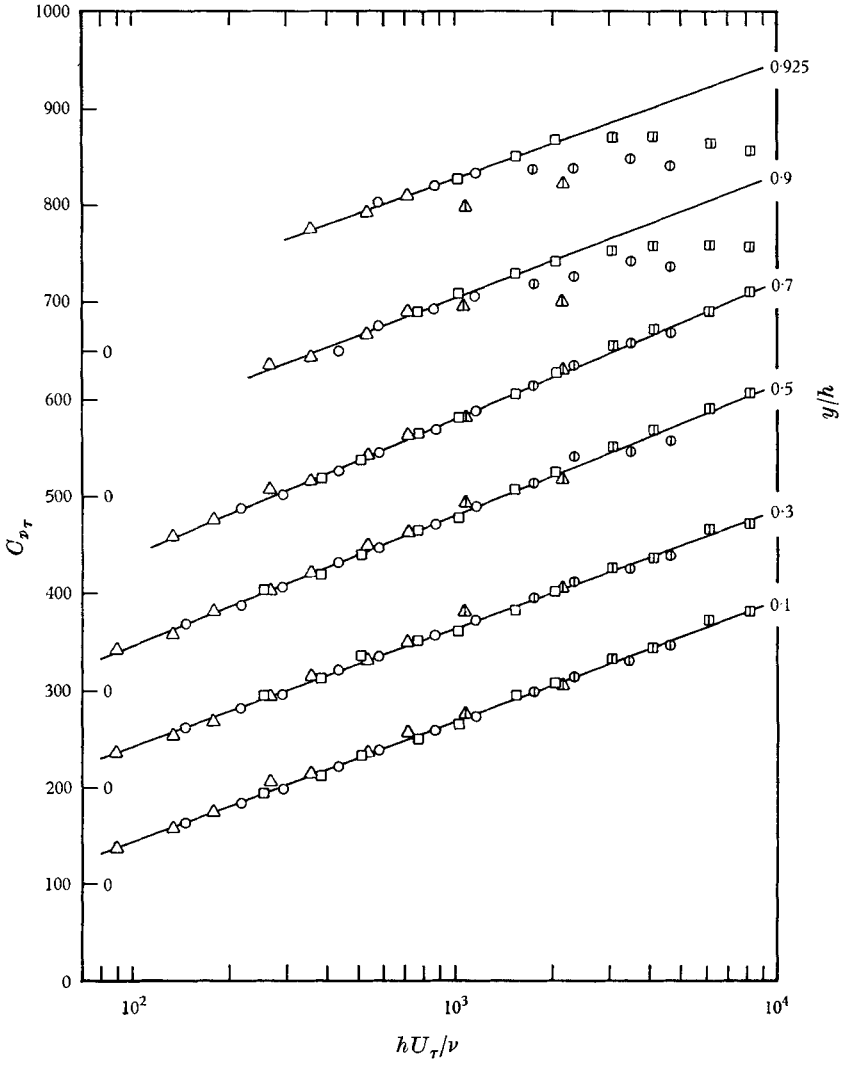

FIGURE 13. Pressure coefficients on upstream face at various values of y/h. □, $U_\tau/U_1 = 0{\cdot}0348$; ○, 0·0360; △, 0·0375. Divided symbols denote $h/\delta > 0{\cdot}5$.

The distributions of the functions g_1 and g_2 were found from the experimental data by plotting C_{p_τ} against $\log_{10}(hU_\tau/\nu)$ for various values of y/h. The results for each value of y/h conformed well to the form of equation (4.24)—see figure 13 for some examples—and the resulting values of g_1 and g_2 are given in figure 14.

For values of y/h less than about 0·8, the pressures followed this wall law over the whole range of h/δ tested. For larger values of y/h, deviations from the wall law occurred for $h/\delta > 0{\cdot}5$, due to the influence of the base pressure. This is

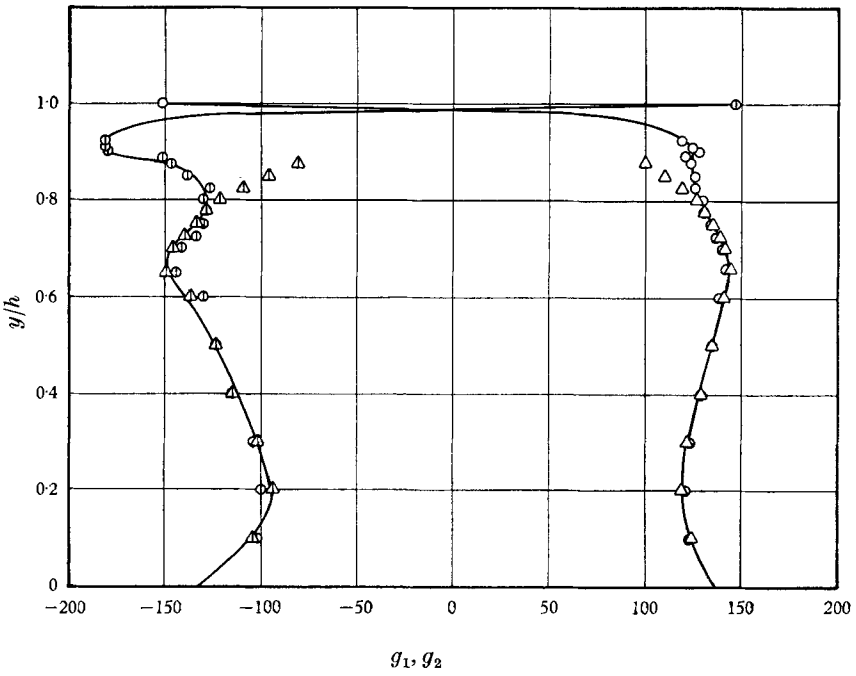

FIGURE 14. Distribution of functions defining shape of pressure distribution on bluff-plate. Values obtained by fitting semi-log lines to data over whole range of h/δ: △, $g_1[y/h]$, ▲, $g_2[y/h]$. Values obtained for $h/\delta < 0{\cdot}5$ only: ○, $g_1[y/h]$; ⊕, $g_2[y/h]$.

demonstrated by the close correspondence between the values of g_1 and g_2 obtained, for $y/h < 0{\cdot}8$, by fitting semi-log lines (*a*) to the points covering the whole range of h/δ, and (*b*) to only those points for which $h/\delta < 0{\cdot}5$. The distortions to the pressure distribution which occur for $y/h > 0{\cdot}8$, when $h/\delta > 0{\cdot}5$, have a negligible effect on the average pressure on the front face however (see figure 9).

The rather irregular shape of the curves in figure 14 seems to reflect a difference between the mechanisms determining the pressures on the plate within the front separation bubble, and outside it.

With the aid of equations (4.16), (4.19) and (4.24), and the information in table 1 and figure 14, the distribution of pressure on a bluff-plate may be predicted from a knowledge of U_τ and δ for the reference profile.

The fairly constant values obtained for the drag coefficient C_{D_m} and the proportionality of drag and base-pressure coefficients in the wall-law region, suggests that the pressure distribution normalized by the maximum pressure should be invariant. A selection of normalized pressure distributions is shown in figure 15, and it can be seen that there are small, but consistent, differences in the distributions, particularly in the region exposed to the front separation bubble. The

shape of the normalized distribution varies with hU_τ/ν, and not with U_1 (or, better, U_τ/U_1) as suggested by Plate.

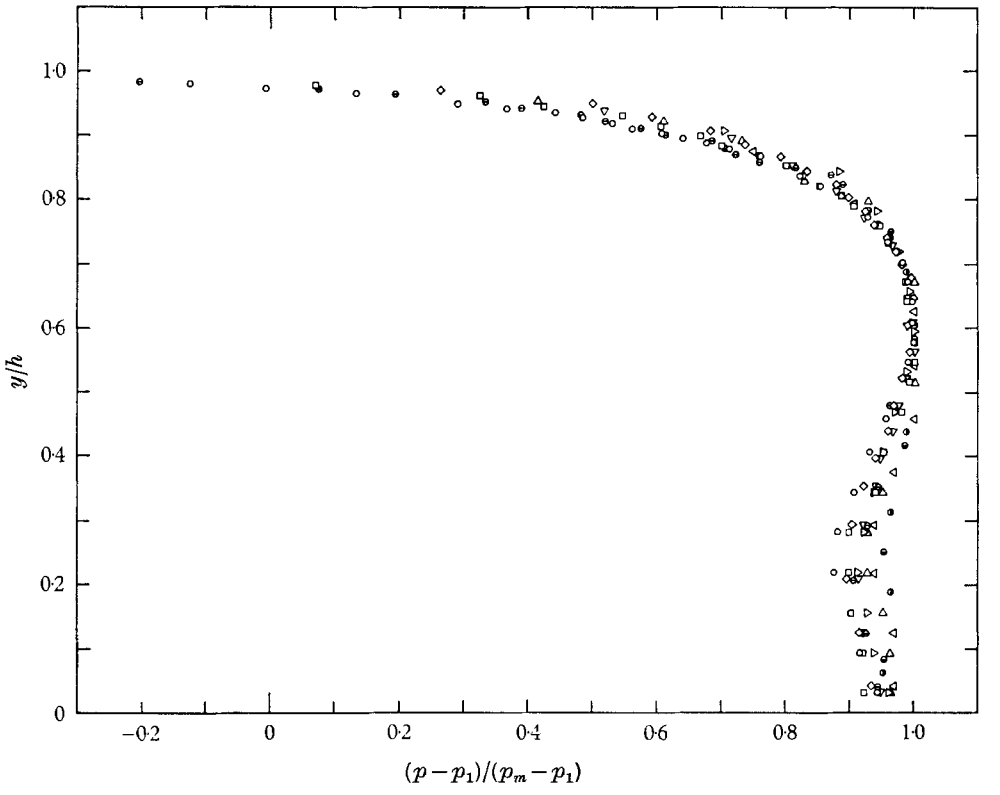

FIGURE 15. A selection of pressure distributions on upstream face of bluff-plate, normalized by maximum pressure.

	h (in.)	U_τ/U_1	$10^{-2}hU_\tau/\nu$	h/δ		h (in.)	U_τ/U_1	$10^{-2}hU_\tau/\nu$	h/δ
◁	$\frac{3}{8}$	0·0375	2·68	0·144	▷	$\frac{1}{2}$	0·0348	10·3	0·219
◑	$\frac{1}{4}$	0·0360	2·91	0·103	⊖	3	0·0375	21·5	1·15
◒	$\frac{3}{16}$	0·0348	3·85	0·082	□	2	0·0360	23·3	0·823
△	1	0·0375	7·16	0·383	◇	$1\frac{1}{2}$	0·0348	30·8	0·658
▽	$\frac{3}{4}$	0·0360	8·73	0·309	○	4	0·0348	82·1	1·75

5. Measurements of flow field

With the smooth wall in the zero pressure-gradient position, and a 4 in. bluff-plate at the 10 ft. 10 in. station, mean-velocity, static-pressure and flow-angle traverses were made at a number of stations in the vicinity of the bluff-plate. The distributions of pressure on the bluff-plate and smooth wall were also measured. The results of these measurements, all made with a reference value of $U_\tau/U_1 = 0{\cdot}0358$, are shown in figure 16.

5.1. *Streamlines*

The values of the non-dimensional stream function ψ/U_1h which were used in drawing the streamlines in figure 16 were obtained by plotting the velocity

profiles in the form shown on the figure, viz.

$$u/U_1 = V\cos\theta/U_1 = f[y/h], \tag{5.1}$$

(where V and θ are the measured magnitude and direction of the local velocity vector), and measuring the integral

$$\psi/U_1 h = \int_0^{y/h} (u/U_1)\, d(y/h). \tag{5.2}$$

When drawing the streamlines use was made of the measured flow angle θ. The locations of the separation and reattachment points were determined (approximately) from surface-shear patterns, and tuft-probe explorations.

5.2. *Displacement surface*

In the highly accelerated flow near the bluff-plate, the usual definition of displacement thickness,

$$\delta^* = \int_0^\infty (1 - u/U_1)\, dy, \tag{5.3}$$

is inadequate. The displacement surface in figure 16 was drawn from values of δ^* obtained by the following method.

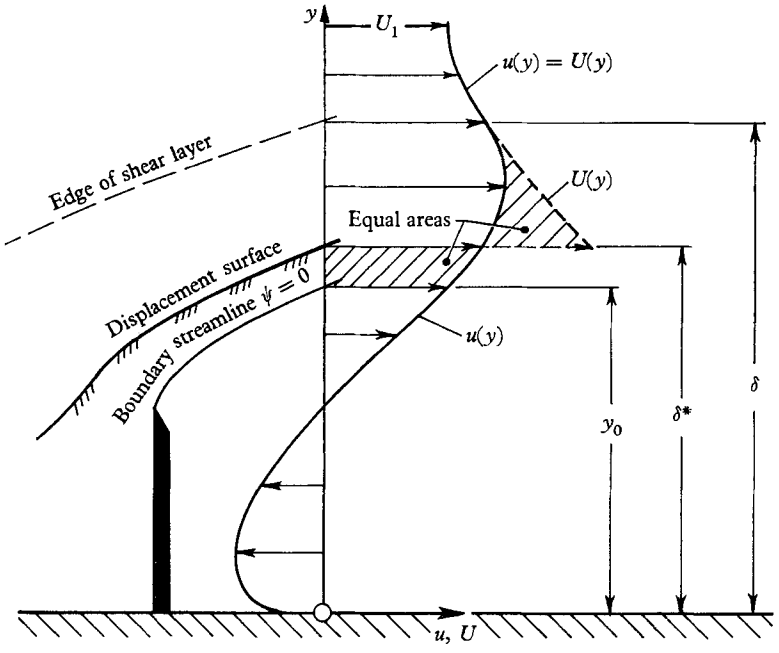

FIGURE 17. Determination of displacement thickness (see text).

Referring to figure 17, let $u(y)$ be the x-component of velocity which is measured in a traverse, and $U(y)$ be the corresponding component in an irrotational, inviscid flow over the displacement surface. Then, outside the shear layer, $u(y) = U(y)$.

The total mass flux through the traverse cross-section is given by

$$\int_0^\infty \rho u\, dy \equiv \int_{\delta^*}^\infty \rho U\, dy. \tag{5.4}$$

The definition of δ^* therefore becomes

$$\int_0^{\delta^*} u\,dy = \int_{\delta^*}^{\infty} (U-u)\,dy, \tag{5.5}$$

or, in the case illustrated where $\int_0^{y_0} u\,dy = 0$,

$$\int_{y_0}^{\delta^*} u\,dy = \int_{\delta^*}^{\infty} (U-u)\,dy. \tag{5.6}$$

To find the distribution of $U(y)$ within the shear layer it was assumed that the measured distributions of static pressure and flow angle would be approximately the same as in the potential flow (for $y > \delta^*$). Thus U was obtained from

$$p + \tfrac{1}{2}\rho(U/\cos\theta)^2 = p_1 + \tfrac{1}{2}\rho U_1^2, \tag{5.7}$$

where p_1 and U_1 are the free-stream static pressure and velocity of the undisturbed flow, and p and θ are the static pressure and flow angle measured in the shear layer. The estimated potential-flow velocity distribution was plotted on the measured profile, and equation (5.6) solved for δ^* by finding the value of y for which the areas shown shaded in figure 17 became equal.

5.3. *Similarity of velocity profiles*

Savage (1960) showed that the velocity profiles measured by Arie & Rouse in the rear separation bubble could be correlated, outside the boundary streamline $\psi = 0$, in the form

$$(u-u_0)/(U_m-u_0) = f[y'/b'], \tag{5.8}$$

where U_m is the velocity at the edge of the shear layer, u_0 is the velocity on the boundary streamline, y' and b' are measured from this streamline, and b' is defined such that $f[y'/b'] = 0{\cdot}5$ at $y'/b' = 1$.

The present results are plotted in this form in figure 18, together with the Goertler (1942) solution for a constant-pressure half-jet (as given by Savage).

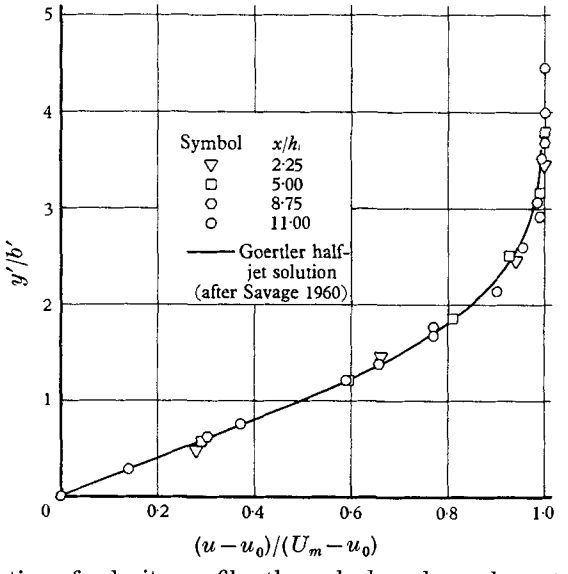

FIGURE 18. Correlation of velocity profiles through shear layer downstream of bluff-plate. $h/\delta = 2{\cdot}34$.

The quite good correlation indicates that the downstream shear flow was largely dominated by the turbulence generated during the initial mixing near the tip of the bluff-plate. For smaller values of h/δ the flow could be expected to be more sensitive to the nature of the upstream boundary layer.

5.4. *Static pressure profiles*

Upstream of the bluff-plate the static pressure varied very little with distance from the wall, except outside the displacement surface. It can be seen from figure 16 that this was true even for the profile through the front separation-bubble at $x/h = -0{\cdot}375$. The downstream profiles, however, exhibit a definite minimum, which occurs at roughly the same distance from the wall in all the profiles, except the one very close to the bluff-plate. Now Arie & Rouse (1956, bluff-plate with downstream splitter) and Tani (1958, down-step) found that the maximum level of turbulence intensity occurred along a surface which was roughly parallel to the wall, and which extended well downstream of the reattachment point. Thus it appears that the pressure minimum found in the present profiles is associated with this region of high turbulence level, and is necessary to balance high values of $\partial(\rho\overline{v'^2})/\partial y$, the gradient of transverse Reynolds stress. As the pressure measurements are uncorrected for turbulence effects, their absolute accuracy is in doubt. However the depression of static pressure in this region cannot be simply a result of instrument errors due to turbulence (see Bradbury 1965 for a discussion of the effect of turbulence on static pressure readings).

6. Pressure-gradient experiments

The smooth wall was tilted into four different positions (the wall positions being referred to as *PG* 1, *PG* 4, *PG* 5 and *PG* 6) to produce distributions of rising pressure. These distributions were measured by the wall pressure taps. Except for the series *PG* 1/1 at the 6 ft. 10 in. station, all drag tests were carried out with U_τ/U_1 held constant at 0·0340, in conformity with the correlation scheme outlined in §2.5.

6.1. *Boundary-layer results*

The main information required from the reference-profile measurements were the values of U_τ/U_1, δ and Π, for use in the correlation scheme, equation (2.11). The parameters U_τ/U_1 and Π were obtained by the means described for the zero pressure-gradient profiles, and δ was taken to be the 99% thickness.

The consistency of the data was confirmed by plotting Δ/δ_{99} against Π, for each of the pressure-gradient profiles, together with a point representing the average of the zero pressure-gradient results. A straight line could be drawn through the points with a scatter of less than $\pm 5\%$ in Π. It was realized later that a consistent measure of the boundary-layer 'thickness' could have been obtained from the other parameters, using Coles's relation

$$\Delta/\delta = (1 + \Pi)/\kappa. \tag{6.1}$$

In fact, the values of δ thus obtained were all feasible measures of the boundary-layer thickness, and $\delta/\delta_{99} > 1$ in every case. However, the independently deduced 99% thickness has been used exclusively in the present work.

The major parameters obtained from the reference profiles are summarized in table 2. In this table, U_1/U_0 is the ratio of the free-stream velocities at the bluff-plate station and the leading edge.

Series	X_1 (ft.)	U_1 (ft./s)	U_1/U_0	U_τ/U_1	δ (in.)	Π
PG 1/1	6·83	53·5	0·926	0·0360	1·82	0·727
PG 1/2	6·83	107·2	0·915	0·0340	1·89	0·774
PG 1/3	10·83	60·0	0·885	0·0340	2·80	0·800
PG 4	10·83	55·2	0·865	0·0340	2·80	0·865
PG 5	10·83	73·5	0·906	0·0340	2·25	0·824
PG 6	10·83	23·4	0·832	0·0340	5·38	0·947

TABLE 2. Reference-profile parameters for pressure-gradient tests

6.2. *Effect of pressure gradients on wall similarity*

From the results of the zero pressure-gradient tests it might be expected that, in pressure gradients too, outer-flow variables like U_1, δ and Π would not be involved in determining the drag when h/δ is small. Thus it was expected that the present results would fit the same wall law, equation (4.8). However, when

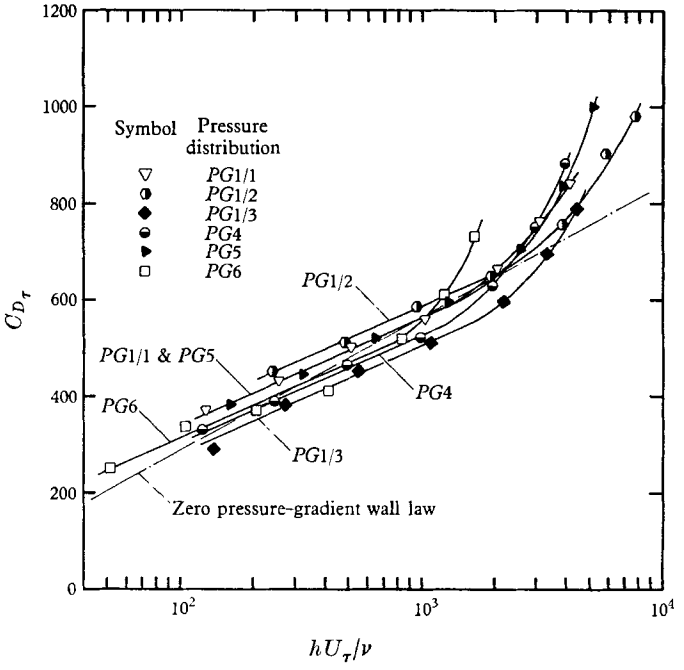

FIGURE 19. Drag coefficients from adverse pressure-gradient tests.

plotted in this form, in figure 19, the results for each pressure distribution produce lines displaced from each other, and from the zero pressure-gradient wall law. Also, the slopes of the semi-log lines are significantly lower (average slope 223) than the slope of the wall law (277).

When considering reasons for these apparent discrepancies it was realized that, in proposing the correlation scheme of equation (2.11), no consideration had been given to the possible effects of the distribution of pressure *downstream* of the bluff-plate on the flow processes in the long, rear separation-bubble, and hence on the base pressure. On further consideration it is apparent that pressure gradients impressed on the downstream flow may affect the development of the shear layer between the main flow and the separated flow. This would affect rates of entrainment of fluid from the bubble, and the distributions of mass- and momentum-flux in the reattaching shear flow. Also the momentum balance in the region of reattachment could be influenced by local pressure gradients.

Unfortunately, the experimental requirement that U_τ/U_1 be held constant at the chosen value of 0·0340 meant that some of the tests had to be carried out at rather low wind-tunnel speeds, with a consequent loss of accuracy in pressure measurements. Because of this, and the limited extent of the data, any further analysis of the results must be speculative. The following discussion is presented, however, because the authors believe the results are highly suggestive, and the implications are worthy of more detailed investigation.

In order to test the hypothesis that pressures on the upstream face of the bluff-plates were determined solely by the wall variables (as in the zero pressure-gradient case), and that the effects of pressure gradients were confined to the base pressure, an attempt was made to separate the upstream and base-pressure components of the drag coefficients obtained at the 10 ft. 10 in. station. There was some difficulty in establishing what portion of the total pressure differential over the bluff-plate was due to pressures on the front face, and what part constituted the base pressure, because the 'ambient' pressure p_1 could not be directly measured at the same time as pressures on the bluff-plate. The procedure adopted was as follows.

The appropriate reference pressure was taken to be the pressure at the bluff-plate station when the plate height was zero. This pressure was measured, and expressed as a pressure coefficient relative to the conditions at an arbitrary datum point far upstream. When the plate height was increased from zero, pressures on the bluff-plate were also expressed as pressure coefficients relative to the upstream datum point. The upstream and base-pressure components of the drag coefficient could then be determined.

The tunnel speed for the distribution *PG* 6 was too low to allow reasonably accurate data reduction for the present purpose. The results obtained for the upstream component of the drag coefficient, for the remaining tests (*PG* 1/3, *PG* 4 and *PG* 5) are shown in figure 20, together with the zero pressure-gradient data. The present results agree quite well with the previous wall law. Note especially that the difference in slopes between the semi-log lines of the two sets of data is eliminated. From these results it would appear that, within the class of boundary layers studied in this investigation, pressures on the upstream face of a bluff-plate are determined by a wall-similarity law, independently of the pressure-gradient history of the boundary-layer. On the other hand, the base pressure appears to be affected by the downstream pressure distribution, even for very small values of h/δ.

In the present experiments, the pressure distribution in the vicinity of the bluff-plate station (when the bluff-plate was absent) could be taken as approximately linear, i.e. $\alpha = (1/\rho)\, dp/dx \simeq$ constant. Then, for small h/δ, it is plausible

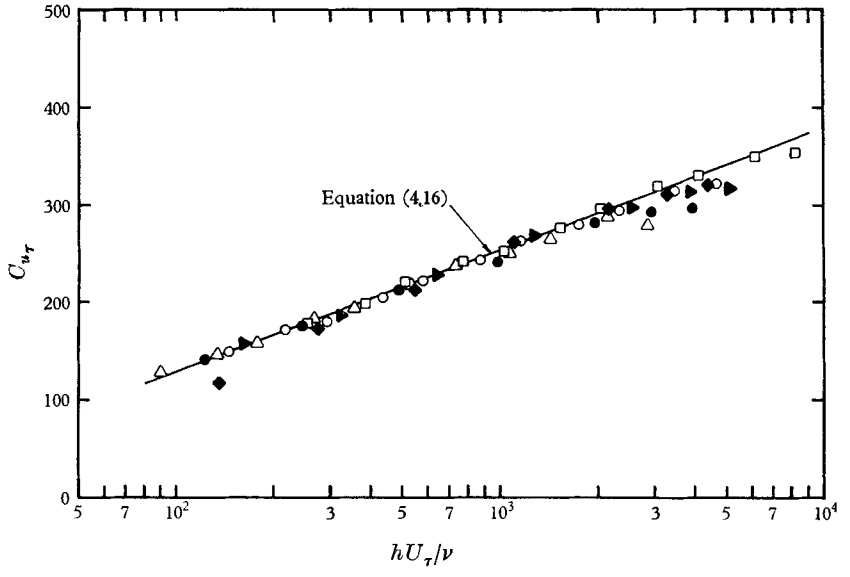

FIGURE 20. Comparison of pressure-gradient data for C_{u_τ} (◆, *PG* 1/3; ●, *PG* 4; ▶, *PG* 5) with zero pressure-gradient results (□, $U_\tau/U_1 = 0{\cdot}0348$; ○, 0·0360; △, 0·0375).

that the upstream flow was characterized solely by h, ρ, μ and U_τ, while the flow in the rear separation-bubble was also affected by α. That is,

$$C_{D_\tau} = f[hU_\tau/\nu,\ \alpha\nu/U_\tau^3], \quad \text{say.} \tag{6.2}$$

From figure 19 it appears that C_{D_τ} varies logarithmically with h in the region covered by (6.2). The semi-log lines in this figure have been drawn with a common slope, because no systematic variation could be detected. However, these conclusions need to be tested with more accurate and extensive data.

According to this interpretation, then, the effect of changing the value of the (approximately constant) downstream pressure gradient is to cause a change in the base-pressure coefficient, ΔC_{b_τ}, which is independent of plate height. This interpretation begs an explanation of the difference in slope between the semi-log lines of the zero pressure-gradient and pressure-gradient data. The authors are unable to advance any satisfactory explanation for this discrepancy. Subject to the validity of the present interpretation of the data, the most likely reason appears to be that the flow in the rear separation-bubble was affected by some extraneous errors in the experimental set-up. Unfortunately, the accuracy of the measurements of the smooth-wall pressure distribution was poor, and no meaningful comparisons of pressure gradients can be made. It is not possible to demonstrate, therefore, that the changes ΔC_{b_τ} in the base-pressure coefficient are uniquely related to $\alpha\nu/U_\tau^3$.

Only tentatively, therefore, the form of equation (6.2) may be refined to

$$C_{D_\tau} = A' \log (hU_\tau/\nu) + B' - \Delta C_{b_\tau}[\alpha\nu/U_\tau^3], \tag{6.3}$$

where A' and B' are presumed to be the same as the constants A and B in the equation for zero pressure-gradient flows, equation (4.11), but are written differently to emphasize the uncertainty as to their true values. The assumptions required to deduce (6.3) from (6.2) are that changes in D/h with changes in plate height are independent of the length scales associated with the viscous sublayer (ν/U_τ), and the downstream pressure gradient (U_τ^2/α).

6.3. *A possible drag-deviation function*

For larger values of h/δ than are covered by equation (6.2), mean velocities and the turbulence structure in the outer part of the boundary layer affect the base pressure. In §2.3 it was suggested that, for quasi-similar boundary layers, the upstream history of the flow might be adequately represented by mean profile parameters like U_τ, U_1, δ and Π. However, the correlation scheme adopted to test this hypothesis, equation (2.11), must be extended to include the effect of the downstream pressure gradient on the base pressure. The revised statement of the hypothesis may be written

$$C_{D_\tau} = f[hU_\tau/\nu,\ h/\delta,\ \Pi,\ \alpha\nu/U_\tau^3]. \tag{6.4}$$

If it is assumed that, for h/δ outside the range of validity of equation (6.3), the effect of α continues to be a constant change in the base-pressure coefficient, $\Delta C_{b_\tau}[\alpha\nu/U_\tau^3]$, the form of variation displayed in figure 19 may be described by

$$C_{D_\tau} + \Delta C_{b_\tau}[\alpha\nu/U_\tau^3] = A' \log (hU_\tau/\nu) + B' + \psi, \tag{6.5}$$

where, according to the hypothesis, the drag-deviation function ψ depends on h/δ and Π only.

It will be recalled that the zero pressure-gradient results demonstrated a marked similarity in the variation of the drag coefficient C_{D_τ} and the velocity ratio U_h/U_τ in the reference profile. Now the velocity ratio in the pressure-gradient profiles may be expressed by

$$U_h/U_\tau = \frac{1}{\kappa} \log \frac{hU_\tau}{\nu} + C + \frac{\Pi}{\kappa} w[h/\delta], \tag{6.6}$$

where Coles's wake function w is a universal function of h/δ. Pursuing the analogy, the further hypothesis could be made that the history of the flow is manifested in similar ways in the mean-velocity and drag-deviation functions. That is, perhaps

$$\psi[\Pi,\ h/\delta] = P[\Pi] . \phi[h/\delta], \tag{6.7}$$

where ϕ is a universal drag-deviation function, and P is a scale factor depending only on Π.

The validity of the assumptions expressed by equations (6.4), (6.5) and (6.7) can be tested by normalizing the value of the deviation function ψ at $h = \delta$,

(i.e. $\psi[\Pi, 1]$) say, for each set of results, to its value when Π has some arbitrary reference value Π', (i.e. $\psi[\Pi', 1]$) say. Then, if the assumptions made are correct, the normalized data should collapse on to a single curve, given by

$$\frac{\psi[\Pi', 1]}{\psi[\Pi, 1]}\psi[\Pi, h/\delta] = \frac{P[\Pi']\phi[1]}{P[\Pi]\phi[1]}P[\Pi]\phi[h/\delta] = P[\Pi']\phi[h/\delta]. \tag{6.8}$$

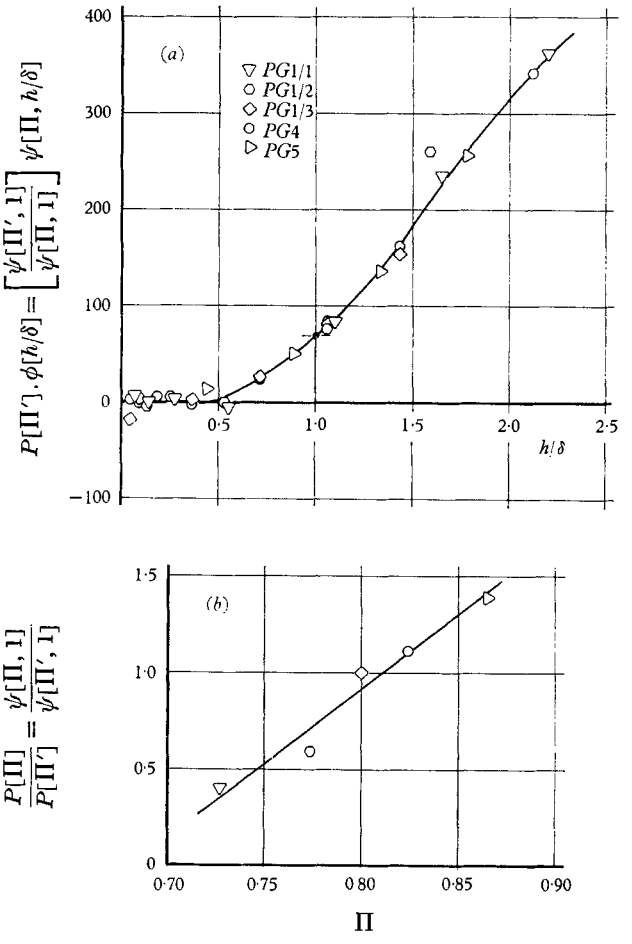

FIGURE 21. A possible universal drag-deviation function. (*a*) Normalized deviations from semi-log lines. (*b*) Correlation of normalizing factor with Π.

The normalizing process described was carried out for all the pressure-gradient data (except those for the distribution *PG* 6, which were too inaccurate for the present purpose), using the data for the distribution *PG* 1/3 to provide the arbitrary reference value Π', with the result shown in figure 21 (*a*). The normalized deviations, when plotted against h/δ, do appear to fall very well on a unique curve. The scale factor P is plotted against Π in figure 21 (*b*), showing a satisfactory correlation.

Thus, encouraging support is obtained for the original hypothesis that the history of the shear flow might be adequately represented by the mean-flow variables U_τ, δ and Π. Also, it appears that this history is manifested in similar ways when mean quantities like velocity (at height h in the reference profile) and pressure (on a bluff-plate of height h immersed in the profile) are determined. Comparison of the proposed form of variation of the drag coefficient,

$$C_{D_\tau} + \Delta C_{b_\tau}[\alpha\nu/U_\tau^3] = A' \log(hU_\tau/\nu) + B' + P[\Pi]\phi[h/\delta], \tag{6.9}$$

with equation (6.6) for the velocity, illustrates this point.

It is tempting to compare the deviation function obtained from these pressure-gradient data with that from the zero pressure-gradient results (table 1). The comparison is hindered by the different slopes of the semi-log lines in the two sets of data. If this difficulty is ignored and the deviations are directly compared, it is found that the shape of the normalized deviation curves agree quite well. However, the scale factor required to match the zero pressure-gradient results with the curve shown in figure 21 (*a*) does not fit into the correlation shown in figure 21 (*b*). Further experiments are required to elucidate the reasons for this discrepancy.

7. Conclusions

The wall-similarity correlation obtained for pressures on the front face of a bluff-plate (which is independent of the pressure-gradient history of the boundary layer, and applies even for $h/\delta > 1$) indicates that the separation process upstream of the bluff-plate is sufficiently rapid to be of the type postulated by Stratford (1959) and Townsend (1960, 1962).

For values of h/δ less than about $\frac{1}{2}$, the flow mechanism in the long rear separation-bubble is also dominated by mean and turbulent velocities characterized by the wall shear stress of the reference profile. That is, in this range of h/δ the base pressure is determined independently of the upstream history of the flow. However, in pressure-gradient flows the base pressure is affected by pressure gradients downstream of the bluff-plate, and so true wall-similarity is not obtained.

For $h/\delta > \frac{1}{2}$ the upstream history of the boundary layer does affect the base pressure, but it appears to be adequately represented by the mean-flow parameters used by Coles (1956) to describe the reference velocity profile. The correlations obtained between the drag coefficient $C_{D_\tau} = D/\frac{1}{2}\rho U_\tau^2 h$ and these parameters appear remarkably similar to the correlations describing the reference velocity profile itself. However, it must be stressed that conclusions derived from the pressure-gradient data are tentative only, as much more detailed experimentation is required to establish the reasons for some inconsistencies in the data.

For zero pressure-gradient flows, the correlations obtained allow the form drag, and, in fact, the actual pressure distribution on the bluff-plate, to be predicted from a knowledge of the thickness and wall shear stress of the reference profile. In adverse pressure-gradient flows, only pressures on the front face may be predicted at this stage.

The authors gratefully acknowledge the assistance given by Dr A. E. Perry, Department of Mechanical Engineering, University of Melbourne, at all stages of the investigation.

REFERENCES

ARIE, M. & ROUSE, H. 1956 *J. Fluid Mech.* **1**, 129.

BRADBURY, L. J. S. 1965 *J. Fluid Mech.* **23**, 31.

CHAPMAN, D. R., KUEHN, D. M. & LARSON, H. K. 1957 *NACA TN* 3869.

CLAUSER, F. H. 1954 *J. Aero. Sci.* **21**, 91.

CLAUSER, F. H. 1956 *Advances in Applied Mechanics* **4**, 16. New York: Academic Press.

COLES, D. 1956 *J. Fluid Mech.* **1**, 191.

GOERTLER, H. 1942 *Z. angew. Math. Mech.* **22**, 244.

GOOD, M. C. 1965 M.Eng.Sc. Thesis, Univ. of Melbourne.

HEAD, M. R. & RECHENBERG, I. 1962 *J. Fluid Mech.* **14**, 1.

HOERNER, S. 1958 *Fluid-Dynamic Drag.* Published by the author.

KORST, H. H. 1956 *J. Appl. Mech., Trans. ASME* E **23**, 593.

MORRIS, H. M. 1954 *Proc. ASCE* **80**, Separate no. 390.

NASH, J. F. & BRADSHAW, P. 1967 *J. Roy. Aero. Soc.* **71**, 44.

NEWMAN, B. G. 1951 *Aust. A.R.C.C. Rept.* no. ACA-53.

PATEL, V. C. 1965 *J. Fluid Mech.* **23**, 185.

PERRY, A. E. & JOUBERT, P. N. 1963 *J. Fluid Mech.* **17**, 193.

PLATE, E. J. 1964 *ASME Paper* no. 64-FE-17.

PRESTON, J. H. 1954 *J. Roy. Aero. Soc.* **58**, 109.

ROSHKO, A. & LAU, J. C. 1965 *Proc. of the 1965 Heat Transfer and Fluid Mech. Inst.*, p. 157.

ROTTA, J. C. 1962 *Progr. Aero. Sci.* **2**, 5. Oxford: Pergamon Press.

SAVAGE, S. B. 1960 *Mech. Engng Res. Lab., Aero. Section, Rept.* no. Ae 3. McGill Univ.

SAWYER, R. A. 1960 *J. Fluid Mech.* **9**, 543.

SAWYER, R. A. 1963 *J. Fluid Mech.* **17**, 481.

SCHLICHTING, H. 1962 *Boundary Layer Theory*, 4th ed. New York: McGraw-Hill.

SCHUBAUER, G. B. & KLEBANOFF, P. S. 1950 *NACA TN* 2133.

SMITH, D. W. & WALKER, J. H. 1958 *NACA TN* 4231.

STRATFORD, B. S. 1959 *J. Fluid Mech.* **5**, 1.

TANI, I. 1958 *Boundary Layer Research*, ed. by H. Goertler, p. 377. Berlin: Springer-Verlag.

TOWNSEND, A. A. 1960 *J. Fluid Mech.* **8**, 143.

TOWNSEND, A. A. 1962 *J. Fluid Mech.* **12**, 536.

TOWNSEND, A. A. 1965*a* *J. Fluid Mech.* **22**, 773.

TOWNSEND, A. A. 1965*b* *J. Fluid Mech.* **22**, 799.

WIEGHARDT, K. 1953 *Forschungshefte für Schiffstechnik* **2**, 65.